Article:

Zhang, J., Li, Q., Kim, K. et al. (2016) On the Performance of Full-duplex Two-way Relay Channels with Spatial Modulation. IEEE Transactions on Communications. p. 1. ISSN: 0090-6778

https://doi.org/10.1109/TCOMM.2016.2600661

On the Performance of Full-duplex Two-way Relay Channels with Spatial Modulation

Jiliang Zhang, *Member IEEE*, Qiang Li*, *Member IEEE*, Kyeong Jin Kim, *Senior Member IEEE*, Yang Wang, Xiaohu Ge, *Senior Member IEEE* and Jie Zhang, *Member IEEE*

***Abstract*—In this paper, the spatial modulation (SM) technique is employed at the source and relay nodes in a full-duplex two-way relay channel (FD-TWRC) to support spectral-efficient bi-directional communications while guaranteeing a low cost implementation. Maximum likelihood (ML) detectors are employed at each node that is subject to an intrinsic self-loop interference (SI). We first propose a tight upper bound on the average bit error probability (ABEP). Then based on the ABEP upper bound, an asymptotic ABEP expression is derived in the high SNR regime. Exploiting the asymptotic ABEP, an exact SNR threshold for the selection between FD-TWRC-SM and half-duplex (HD)-TWRC-SM is derived in a closed form, which sheds light on when it is beneficial to select the FD (or HD) mode. In addition, the power allocation (PA) among sources and relay is investigated, through which an optimal PA factor in terms of ABEP is obtained. All analytical results derived in this paper are verified by Monte Carlo simulations, from which some new insights are obtained on the performance of FD-TWRC-SM.**

***Index Terms*—Two-way relay channel, full-duplex relay, spatial modulation, self-loop interference.**

I. INTRODUCTION

Multi-antenna techniques are widely accepted as a key enabler in achieving a high data rate and spectral efficiency in the next generation of communications. However, a significant amount of power is consumed for transmitting signal [1], especially when multiple transmit antenna elements work simultaneously due to the same number of transmit radio frequency (RF) chains. Driven by this, the spatial modulation (SM) technique has been proposed to reduce the cost of the multi-antenna systems [2]–[6]. The performance of SM systems with multiple antennas has been evaluated through analytical analysis [7]–[12] and measurement [13]–[16].

The SM technique has been applied to various relay systems [17]–[27]. A relay system employing SM, which utilizes the relay-selection information to achieve a higher throughput is proposed in [17]. In [18], the performance of the dual-hop space shift keying (SSK) system is evaluated. A dual-hop SM system is proposed and analyzed in [19]. A two-hop space-time shift keying (STSK) relay system is introduced and its performance is analyzed in [20]. In [21], the authors analyzed the distributed SSK in relay-aided uplink cellular networks. Furthermore, the authors in [22] analyzed the performance of SSK relay systems with multiple cooperative relays considering both amplify-and-forward (AF) and decode-and-forward (DF) protocols. A bit error probability analysis of SSK in DF relay channels with best relay selection is conducted in [23]. In [24], the authors proposed a distributed SM system for multi-relay networks whose diversity was analyzed analytically. In addition, the authors in [25] proposed a differential SM for dual-hop AF relaying system. A framework to analyze the average bit error probability (ABEP) of the SM system with a single-antenna AF node was proposed in [26]. The authors in [27] proposed an SM based cooperative diversity protocol where the network nodes act as relays to help forward the source data, while transmitting their own data.

However, all these existing work above considered only half-duplex (HD) relays, which have to transmit and receive signals in orthogonal channels. Driven by the inherent spectrum inefficiency suffered by HD relay systems, there has been an increasing interest in full-duplex (FD) relays that are capable of transmitting and receiving signals in the same frequency band simultaneously, e.g., [28] and the references therein. Although a substantially higher spectrum efficiency can be promised by the FD relay system, the self-loop interference (SI) that leaks between the transmit and receive antennas of the FD relay node needs to be carefully addressed [29]. Inspired by the benefits of FD transmissions, some recent work has investigated FD-SM transmission in none cooperative relay systems, e.g., [30]–[32].

The impact of SI on the two-way relay channel (TWRC) with a FD relay, which is a spectral-efficient transmission protocol for wireless networks, has been investigated in [33]–[38]. It is shown that when SI is weak enough, the TWRC with the FD relay achieves a higher spectral efficiency than the TWRC with the HD relay. On the other hand, the performance of the HD-TWRC with SM has been investigated in [39]–[41]. Motivated by the promising performance of the TWRC

Jiliang Zhang and Yang Wang are with Shenzhen Graduate School, Harbin Institute of Technology, Shenzhen, P. R. China. e-mail: {zhangjiliang,wangyang}@hitsz.edu.cn. Qiang Li and Xiaohu Ge are with School of Electronic Information and Communications, Huazhong University of Science and Technology, Wuhan, P. R. China. e-mail: {qli_patrick, xhge}@hust.edu.cn. Kyeong Jin Kim is with Mitsubishi Electric Research Lab (MERL), Cambridge, MA, USA. e-mail: kyeong.j.kim@hotmail.com. Jie Zhang is with Department of Electronic and Electrical Engineering, University of Sheffield, UK. e-mail: jie.zhang@sheffield.ac.uk.

The research is funded in part by National Natural Science Foundation of China (61501137), by Science and Technology Basic Research Project of Shenzhen (JCYJ20140417172417169, JCYJ20150513151706577), by the Fundamental Research Funds for the Central Universities under the grant (2015XJGH011), and by WiNDOW, a research project supported by the European Commission under its 7th Framework Program (318992).

This research is supported by the Key Laboratory of Network Oriented Intelligent Computation, the Short-Range Wireless Interconnection Industry Public Service Platform, the National International Scientific and Technological Cooperation Base of Green Communications and Networks (2015B01008), and Hubei International Scientific and Technological Cooperation Base of Green Broadband Wireless Communications.

* Correspondence Author.

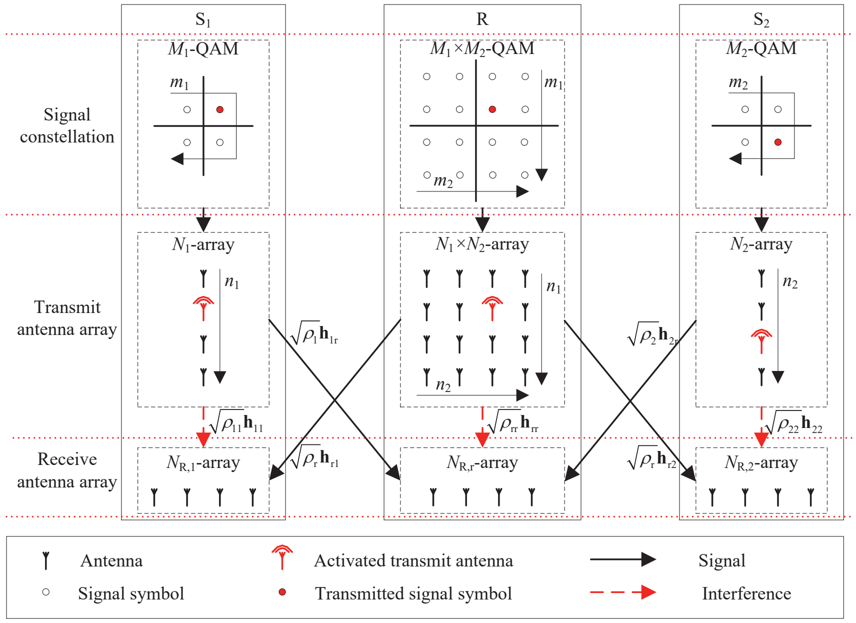

Fig. 1. System model of the considered FD-TWRC-SM with 4 bits per channel use (bpcu).

and FD relaying, in this paper we consider a FD TWRC with SM performed at each node to support the bi-directional communications between two end users, which is referred to as FD-TWRC-SM as illustrated in Fig. 1. The main contributions of this paper are summarized as follows:

1) A FD-TWRC-SM system is proposed and investigated to enhance the system spectral efficiency. To the best of our knowledge, this is the first attempt to apply SM techniques to the TWRC with FD relaying in the literature.
2) Taking into account the impact of the residual SI, an analytical pairwise error probability (PEP) and a tight upper bound on the ABEP of the FD-TWRC-SM are respectively obtained in closed forms. On this basis, we find that the diversity order of FD-TWRC-SM significantly depends on the quality of the SI cancellation.
3) Comparisons between HD-TWRC-SM and FD-TWRC-SM schemes are conducted to provide insights into the selection between FD and HD modes. Under a given strength of SI cancellation, an exact signal-to-noise ratio (SNR) threshold, below which the FD-TWRC-SM outperforms the HD-TWRC-SM in terms of the ABEP, is analytically derived.
4) A power allocation (PA) scheme is applied that allocates different transmit powers to all nodes subject to a sum power constraint. The optimal PA factor that leads to the best ABEP is derived in a closed form.
5) All analytical results are verified through numerical results and employed to analyze the system performance of FD-TWRC-SM under various conditions. Some useful insights are obtained regarding the performance of FD-TWRC-SM.

The remainder of this paper is organized as follows. In Section II, the system model of FD-TWRC-SM is introduced. In Section III, an analytical union upper bound on the ABEP is obtained. Then in Section IV, the proposed ABEP upper bound is employed to evaluate the system performance of FD-TWRC-SM. Simulation results are provided in Section V to demonstrate the effectiveness of the proposed FD-TWRC-SM. Finally, Section VI concludes this paper.

II. SYSTEM MODEL OF FD-TWRC-SM

We consider a FD-TWRC-SM with DF relaying protocol at the relay node that is similar to the TWRC with the FD relaying in [38]. As shown in Fig. 1, the system consists of two source nodes denoted by $\mathrm{S}_i, i = 1, 2$, and one FD relay node denoted by R, where S_1 and S_2 want to exchange information with the help of R. There is no direct link between the two sources due to a very large distance between them [42]. All S_1, S_2, and R transmit signals using the SM scheme. In an SM transmission, S_1 and S_2 are respectively equipped with N_1 and N_2 transmit antennas and only a single transmit antenna in the transmit antenna array of each node is activated. The index of the activated transmit antenna is employed to carry a block of bits to increase the overall spectral efficiency. On the other hand, $N_{\mathrm{R},1}$, $N_{\mathrm{R},2}$, and $N_{\mathrm{R},r}$ receive antennas are respectively equipped at S_1, S_2, and R to perform the maximum likelihood (ML) detection. A detailed design of SM transceivers can be found in [2].

Without loss of generality, we consider a wireless fading channel that remains static within a period of a time block of symbols but changes independently from one time block to another [34], [43]–[47]. $\mathbf{h}_{ir}[k, n_i]$ denotes the channel amplitudes from the n_ith transmit antenna of S_i to all receive antennas at R in the kth time block and $\mathbf{h}_{ri}[k, n_r]$ denotes the channel amplitudes from the n_rth transmit antenna of R to all receive antennas at S_i in the kth time block. Both source nodes and the relay node are full duplex and suffered from SI. All channel amplitudes follow independent and identically distributed (i.i.d.) Rayleigh distributions. The transmit SNRs

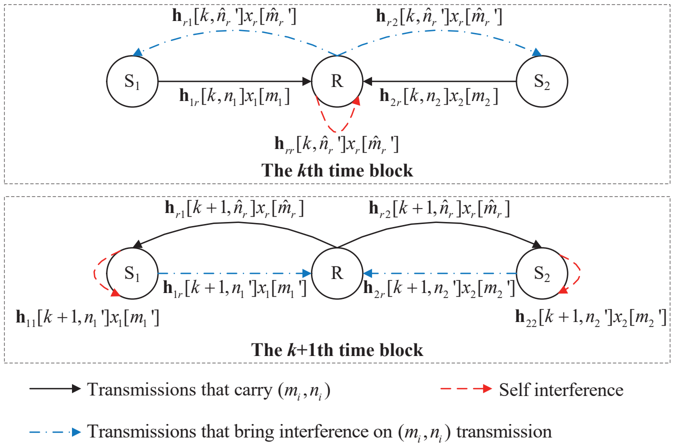

Fig. 2. Intended signal and interference signal for the information transmitted in the kth time slot.

at the source and the relay node are denoted by ρ_i and ρ_r, respectively. The SI cancellation can be performed using passive or active cancellation techniques [48]–[50]. Although the SI can be effectively mitigated by existing methods, perfect SI cancellation cannot be guaranteed in practical implementations. Thus, a remaining residual SI at the receive antenna of the FD node always exists. After SI cancellation, $\mathbf{h}_{ii}[k,n_i]$ denotes the SI channel amplitudes at S_i from its n_ith transmit antenna to all receive antennas, and $\mathbf{h}_{rr}[k,n_r]$ denotes the SI channel amplitudes at R. $\mathbf{h}_{ii}$ and $\mathbf{h}_{rr}$ follow i.i.d. Rayleigh distributions and the interference to noise ratio (INR) at S_i and R are respectively denoted as ρ_{ii} and ρ_{rr}.

In the state of the art works, the characterization of the residual SI has been modelled either as a random variable that has a constant signal to interference ratio (SIR), i.e., $\rho_{ii} = \beta_i\rho_i$ and $\rho_{rr} = \beta_r\rho_r$ [51] or a random variable that is scaled with the transmit SNR by a factor $0 \le \mu \le 1$ where $\rho_{ii} = \rho_i^{1-\mu}$ and $\rho_{rr} = \rho_r^{1-\mu}$, respectively [34], [42], [43], [52]–[55]. In general, these two models are equivalent for analytical derivation by letting $\mu = 1 - \log_{\rho_i}\beta_i\rho_i$ and $\mu = 1 - \log_{\rho_r}\beta_r\rho_r$. However, the model with μ can provide important insights on the fundamental properties of FD-TWRC-SM systems, e.g., diversity orders and SNR gaps. Although there are some previous work that focus on the FD SM system, they either model the remaining residual SI as a complex Gaussian variable with a variance [31], [32] or assume that the SI can be cancelled completely [30]. In the absence of any research on the modeling of the residual SI in the SM context, in this paper, we generally use $\rho_{ii} = \rho_i^{1-\mu}$ and $\rho_{rr} = \rho_r^{1-\mu}$, respectively. The constant SIR model will also be briefly discussed in Section V.

In general, the transmission of each block of information $I_i \triangleq (m_i, n_i)$ is carried out in two time blocks. In the first time block, both S_is transmit $I_i = (m_i, n_i)$ to R, and R detects the information as $\hat{I}_i \triangleq (\hat{m}_i, \hat{n}_i)$. In the second time block, R transmits $\hat{I}_i = (\hat{m}_i, \hat{n}_i)$ to both S_is, and S_is detect the information as $\check{I}_i \triangleq (\check{m}_i, \check{n}_i)$. From the visual angle of I_i transmitted at the kth time block, interference in both time blocks are shown in Fig. 2. In the kth time block, S_is transmit the m_ith M_i-quadrature-amplitude modulation (QAM) symbol through the n_ith transmit antenna simultaneously to R using the SM transmission scheme. The relay R, with one-block processing delay, broadcasts the received information blocks in the previous time block $k-1$, which is denoted as $(\hat{m}_r', \hat{n}_r')$, to the sources simultaneously, thus causing a SI.

The received signal $\mathbf{y}_r[k]$, consisting of the received signal at each receive antenna at R in the kth time block, is composed of the signal $x_1[m_1]$ that is transmitted over channel from S_1 to R, the signal $x_2[m_2]$ that is transmitted over channel from S_2 to R, the SI $\sqrt{\rho_r^{1-\mu}}\mathbf{h}_{rr}[k,\hat{n}_r]x_r[\hat{m}_r']$, and noise $\mathbf{w}_r[k] \sim \mathcal{CN}(0,\sigma_r^2)$ as (1).

In this paper, we consider SM schemes with QAM signal constellations at each node. The signal constellation of the phase-shift-keying (PSK) SM can be readily obtained following the same steps of the QAM SM and is thus omitted here. Without loss of generality, we assume that S_i has N_i transmit antennas and an M_i-QAM signal constellation diagram, R has N_r transmit antennas and an M_r-QAM signal constellation diagram. Benefited from the SM scheme, even though a large scale antenna array is equipped at the relay node, we need only one transmit RF chain and therefore the power consumption and the receive complexity of the system is acceptable. For tractable analysis, we restrict that $M_r = M_1M_2$ and $N_r = N_1N_2$, and assume that the signals transmitted by both sources in the first hop are Gray coded. In the $k+1$th time block, at the relay node, the information from both source nodes are estimated, i.e., $\hat{n}_1$, $\hat{n}_2$, $\hat{m}_1$, and $\hat{m}_2$. Then the relay node activates the $\hat{n}_r = \hat{n}_1 + (\hat{n}_2 - 1)N_1$th antenna to transmit the signal $x_r[\hat{m}_r] = x_r[\hat{m}_1 + (\hat{m}_2 - 1)M_1]$ that corresponds to the $\hat{m}_1$th row and the $\hat{m}_2$th column of the M_r-QAM signal constellation diagram. That is, the estimated symbols $\hat{m}_1$ and $\hat{m}_2$ are interpreted as the Quadrature and In-phase components respectively, which are then used to locate the transmitted symbol by the relay. Simultaneously, the sources transmit (m_i', n_i') to the relay R and cause a SI. Thus, the received signal at S_i in the subsequent time block $k+1$ is given as (2), where $\mathbf{w}_i[k] \sim \mathcal{CN}(0,\sigma_i^2)$. Without loss of generality, we assume that $\sigma_i^2 = \sigma_r^2 = \sigma^2$. The optimal detector based on the ML principle is deployed at each node. We assume that the exact instantaneous channel state information (CSI) and perfect time synchronization are available at the receiver side, as in [2], [7], [8]. According to (1), we have (3), and the principle of the ML receiver is to find out $(\hat{n}_1, \hat{n}_2, \hat{m}_1, \hat{m}_2)$ to maximize the likelihood function, i.e., (4). Following the approaches in [8, Section III-A] and [7, Section II-C], the ML detector at R is represented as (5), where $\|\cdot\|^2$ is the 2-norm of a vector.

Assuming that the sources are equipped with buffers, each

$$\mathbf{y}_r[k] = \underbrace{\sqrt{\rho_1}\mathbf{h}_{1r}[k,n_1]x_1[m_1]}_{\text{Received from } \mathrm{S}_1} + \underbrace{\sqrt{\rho_2}\mathbf{h}_{2r}[k,n_2]x_2[m_2]}_{\text{Received from } \mathrm{S}_2} + \underbrace{\sqrt{\rho_r^{1-\mu}}\mathbf{h}_{rr}[k,\hat{n}_r']x_r[\hat{m}_r']}_{\text{Loop Interference}} + \underbrace{\mathbf{w}_r[k]}_{\text{Noise}} \quad (1)$$

source is aware of its own transmitted message in the previous time block. Specifically, since (n_2, m_2) was transmitted by S_2 and stored in the buffer at S_2, a simple self-interference cancellation can be performed by S_2 to eliminate the uncertainty of (n_2, m_2). Then the set of candidate $(\check{n}_r, \check{m}_r)$ can be narrowed to $(\check{n}_1 + (n_2-1)N_1, \check{m}_1 + (m_2-1)M_1)$. Thus, the detection process at S_2 is given by (6). A similar detection process is applied to S_1.

Note that the original symbols denote the actual message that is transmitted. Symbols with $\hat{\cdot}$ denote the messages estimated by the detector at R, whereas symbols with $\check{\cdot}$ denote the messages estimated by the detector at the sources. These notations are also applied to the antenna indices n_i and signal indices m_i.

III. ABEP Upper Bound

In this section, we analyze the error performance of the TWRC-SM analytically. For arbitrary MIMO systems, the analysis of the exact ABEP is almost intractable due to the complex multidimensional integrals. Instead, the union upper bound technique is widely used to calculate the ABEP upper bound based on PEP [7, Eq. (3)], [8, Eq. (5)]. If the analytical PEP can be obtained, an upper bound on the ABEP of the information transmission from S_1 to S_2 via R is given by (7), where $I_i \triangleq (m_i, n_i)$ denotes the transmitted message from S_i. $PEP\,(m_1, n_1; \check{m}_1, \check{n}_1 | m_2, n_2)$ denotes the probability of choosing the wrong symbol $\check{I}_1$ assuming that there are only two symbols (I_1 and $\check{I}_1$) possibly being transmitted. $D_{\mathrm{H}}\,(\check{n}_1, \check{m}_1, n_1, m_1)$ denotes the Hamming distance between $\check{I}_1$ and I_1.

Moreover, the pairwise error $I_1 \to \check{I}_1$ may occur under any possible $\hat{I}_i$ that is detected by R. Therefore, according to the total probability theorem, we have (8), where $PEP\,(m_1, n_1; \hat{m}_1, \hat{n}_1, \hat{m}_2, \hat{n}_2; \check{m}_1, \check{n}_1 | m_2, n_2) \triangleq \Pr(\check{I}_1 | \hat{I}_1, \hat{I}_2, I_2) \Pr(\hat{I}_1, \hat{I}_2 | I_1, I_2)$ is defined as the probability of choosing the wrong symbol $(\check{n}_1, \check{m}_1)$ assuming that there are only two symbols (I_1 and $\check{I}_1$) possibly being transmitted under the condition that $(\hat{m}_1, \hat{n}_1, \hat{m}_2, \hat{n}_2)$ is decided at R. Therefore, a union upper bound on the ABEP of TWRC-SM is computed by (9).

As discussed in [56] and the references therein, in TWRC systems, the ABEP is dominated by the hop having a worse performance. Based on this idea, we give a framework for analyzing and evaluating the performance of TWRC-SM systems and propose an upper bound on the ABEP by dividing the summations in (9) into three cases and compute them separately. The new upper bound on the ABEP of the information transmission from S_1 to S_2 is summarized in Proposition 1. Note that the ABEP upper bound of the information transmission from S_2 to S_1 can be similarly obtained.

Proposition 1. *The ABEP of TWRC-SM is upper bounded as (10), where $ABEP_{\hat{I}_2 \neq I_2}$, $ABEP_{\hat{I}_1 \neq I_1, \hat{I}_2 = I_2}$, and $ABEP_{\hat{I}_1 = I_1, \hat{I}_2 = I_2}$ are respectively defined as (11)-(13). In Eqs. (11)-(13), $PEP_{1\mathrm{r}}(m_1, n_1, m_2, n_2; \hat{m}_1, \hat{n}_1, \hat{m}_2, \hat{n}_2)$ denotes the PEP of the first hop; the probability of choosing the symbol $(\hat{I}_1, \hat{I}_2)$ assuming that there are only two symbols, (I_1, I_2) and $(\check{I}_1, \check{I}_2)$, possibly being transmitted. $PEP_{\mathrm{r}2}(\hat{m}_1, \hat{n}_1, \hat{m}_2, \hat{n}_2; \check{m}_1, \check{n}_1\ | m_2, n_2)$ denotes the PEP of the second hop; the probability of choosing the symbol $\check{I}_1$ assuming that there are only two symbols, $(\hat{I}_1, \hat{I}_2)$ and $(\check{I}_1, \check{I}_2)$, possibly being transmitted where I_2 is known a priori.*

Proof: See Appendix A. ■

Proposition 1 provides a framework to derive the analytical upper bound on the ABEP of TWRC-SM systems by giving

$$\mathbf{y}_i[k+1] = \underbrace{\sqrt{\rho_r}\mathbf{h}_{ri}[k+1, \hat{n}_r]x_r[\hat{m}_r]}_{\text{Desired Signal}} + \underbrace{\sqrt{\rho_i^{1-\mu}}\mathbf{h}_{ii}[k+1, n_i']x_i[m_i']}_{\text{Loop Interference}} + \underbrace{\mathbf{w}_i[k+1]}_{\text{Noise}} \tag{2}$$

$$\mathbf{y}_r[k] \sim \mathcal{CN}(\sqrt{\rho_1}\mathbf{h}_{1r}[k, n_1]x_1[m_1] + \sqrt{\rho_2}\mathbf{h}_{2r}[k, n_2]x_2[m_2], \rho_r^{1-\mu}|x_r[\hat{m}_r']|^2 + 1) \tag{3}$$

$$(\hat{n}_1, \hat{n}_2, \hat{m}_1, \hat{m}_2) = \underset{\hat{n}_1, \hat{n}_2, \hat{m}_1, \hat{m}_2}{\arg\max} \left\{ \frac{e^{-\frac{\|\mathbf{y}_r - \sqrt{\rho_1}\mathbf{h}_{1r}[k, \hat{n}_1]x_1[\hat{m}_1] - \sqrt{\rho_2}\mathbf{h}_{2r}[k, \hat{n}_2]x_2[\hat{m}_2]\|^2}{2(\rho_r^{1-\mu}|x_r[\hat{m}_r']|^2 + 1)}}}{[2\pi(\rho_r^{1-\mu}|x_r[\hat{m}_r']|^2 + 1)]^{\frac{N_{\mathrm{R},r}}{2}}} \right\} \tag{4}$$

$$(\hat{n}_1, \hat{n}_2, \hat{m}_1, \hat{m}_2) = \underset{\hat{n}_1, \hat{n}_2, \hat{m}_1, \hat{m}_2}{\arg\min} \; \{\|\mathbf{y}_r - \sqrt{\rho_1}\mathbf{h}_{1r}[k, \hat{n}_1]x_1[\hat{m}_1] - \sqrt{\rho_2}\mathbf{h}_{2r}[k, \hat{n}_2]x_2[\hat{m}_2]\|^2\} \tag{5}$$

$$(\check{m}_1, \check{n}_1) = \underset{\{\check{n}_1, \check{m}_1\}}{\arg\min}\{|\mathbf{y}_2 - \sqrt{\rho_r}\mathbf{h}_{r2}\,[k+1, \check{n}_1 + (n_2-1)N_1]\,x_r\,[k+1, \check{m}_1 + (m_2-1)M_1]\,|\} \tag{6}$$

$$ABEP \le \frac{\sum\limits_{I_1=(1,1)}^{(M_1,N_1)} \sum\limits_{I_2=(1,1)}^{(M_2,N_2)} \sum\limits_{\check{I}_1=(1,1)}^{(M_1,N_1)} D_{\mathrm{H}}\,(\check{n}_1, \check{m}_1, n_1, m_1)\,PEP\,(m_1, n_1; \check{m}_1, \check{n}_1 | m_2, n_2)}{N_1 N_2 M_1 M_2 \log_2(N_1 M_1)} \tag{7}$$

$$PEP\,(m_1, n_1; \check{m}_1, \check{n}_1 | m_2, n_2) = \sum_{\hat{I}_1=(1,1)}^{(M_1,N_1)} \sum_{\hat{I}_2=(1,1)}^{(M_2,N_2)} PEP\,(m_1, n_1; \hat{m}_1, \hat{n}_1, \hat{m}_2, \hat{n}_2; \check{m}_1, \check{n}_1 | m_2, n_2) \tag{8}$$

$$ABEP \le \frac{\sum\limits_{I_1=(1,1)}^{(M_1,N_1)} \sum\limits_{I_2=(1,1)}^{(M_2,N_2)} \sum\limits_{\hat{I}_1=(1,1)}^{(M_1,N_1)} \sum\limits_{\hat{I}_2=(1,1)}^{(M_2,N_2)} \sum\limits_{\check{I}_1=(1,1)}^{(M_1,N_1)} D_{\mathrm{H}}\,(\check{n}_1, \check{m}_1, n_1, m_1)\,PEP\,(m_1, n_1; \hat{m}_1, \hat{n}_1, \hat{m}_2, \hat{n}_2; \check{m}_1, \check{n}_1 | m_2, n_2)}{N_1 N_2 M_1 M_2 \log_2(N_1 M_1)} \tag{9}$$

PEP_{1r} and PEP_{r2} in closed forms. For the FD-TWRC-SM systems, $PEP_{\mathrm{FD,1r}}$ and $PEP_{\mathrm{FD,r2}}$ are derived in Lemma 1 and Lemma 2, respectively. For the HD-TWRC-SM systems, $PEP_{\mathrm{HD,1r}}$ and $PEP_{\mathrm{HD,r2}}$ are derived in Lemma 3.

Lemma 1. *The PEP of the first hop transmission from* S_1 *and* S_2 *to R in an FD-TWRC-SM system is computed as follows:*

$$PEP_{\mathrm{FD,1r}} = \frac{\sum\limits_{\hat{m}'_r=1}^{M_1 M_2} \mathcal{R}(N_{\mathrm{R},r}, \upsilon)}{M_1 M_2}, \tag{14}$$

where υ *is computed by (15),* $\mathcal{R}(\kappa, N_{\mathrm{R}}) \triangleq [\frac{1}{2}(1 - \sqrt{\frac{\kappa}{\kappa+1}})]^{N_{\mathrm{R}}} \sum\limits_{q=0}^{N_{\mathrm{R}}-1} C^{q}_{N_{\mathrm{R}}-1+q}[\frac{1}{2}(1+\sqrt{\frac{\kappa}{\kappa+1}})]^{q}$*, and* C_n^k *denotes the binomial coefficient indexed by* n *and* k*.*

Proof: See Appendix B. ∎

Lemma 2. *The PEP of the second hop transmission from R to* S_2 *in an FD-TWRC-SM system is computed as follows:*

$$PEP_{\mathrm{FD,r2}} = \frac{\sum\limits_{m'_2=1}^{M_2} \mathcal{R}(N_{\mathrm{R},2}, \xi)}{M_2}, \tag{16}$$

where ξ *is defined as (17).*

Proof: Since the residual SI and the noise are both complex Gaussian distributed with variances of $\rho_2^{1-\mu}$ and 1, respectively, the transmission from R to S_2 is equivalent to the SM transmission with an average SNR of $\rho_{\mathrm{e},r2} = \frac{\rho_r}{\rho_2^{1-\mu}|x_i[m'_2]|^2+1}$. Similar to the derivations in Appendix B, we have $PEP_{\mathrm{r2},\mathbf{h}_{r2}} = Q(\sqrt{\|\mathbf{d}_{r2}\|^2/2})$, where $\mathbf{d}_{r2}$ is defined as (18), and $Q(x) \triangleq \frac{1}{\sqrt{2\pi}}\int_x^\infty e^{\frac{u^2}{2}}\mathrm{d}u$ is the tail probability of the standard normal distribution[1]. Following the steps of (55)-(58), we obtain (16). ∎

Lemma 3. *For HD-TWRC-SM systems,* $PEP_{\mathrm{HD,1r}}$ *and* $PEP_{\mathrm{HD,r2}}$ *are respectively derived as*

$$PEP_{\mathrm{HD,1r}} = \mathcal{R}(N_{\mathrm{R},r}, \upsilon_{\mathrm{HD}}), \tag{19}$$

$$PEP_{\mathrm{HD,r2}} = \mathcal{R}(N_{\mathrm{R},2}, \xi_{\mathrm{HD}}), \tag{20}$$

where υ_{HD} *and* ξ_{HD} *are respectively given in Eqs. (21) and (22).*

Proof: Since there is no SI in the HD-TWRC-SM, by substituting $x_r[\hat{m}'_r] = 0$ and $x_2[m'_2] = 0$ into (15) and (17) respectively, we obtain (19) and (20) by simple algebraic manipulations based on (14) and (16). ∎

IV. Performance Analysis

In this section, we analyze the system performance of the TWRC-SM systems over i.i.d. Rayleigh fading channels. Especially, we will first obtain asymptotically tight performance bounds that provide insights on the fundamental properties of FD-TWRC-SM systems. And then we will develop an optimal FD and HD switching scheme in TWRC-SM systems. To this, a corresponding decision threshold will be given as the root of a polynomial equation.

A. Asymptotic ABEP and diversity order

We first derive an asymptotic ABEP of the FD-TWRC-SM transmission from S_1 to S_2 in the following Proposition 2.

[1] Due to space limitations, we omit the detailed derivation.

$$ABEP \le ABEP_{\hat{I}_2 \ne I_2} + ABEP_{\hat{I}_1 \ne I_1, \hat{I}_2 = I_2} + ABEP_{\hat{I}_1 = I_1, \hat{I}_2 = I_2} \tag{10}$$

$$ABEP_{\hat{I}_2 \ne I_2} = \frac{\sum\limits_{m_1=1}^{M_1}\sum\limits_{m_2=1}^{M_2}\sum\limits_{\hat{I}_1=(1,1)}^{(M_1,N_1)}\sum\limits_{\hat{I}_2 \ne I_2=(1,1)}^{(M_2,N_2)} PEP_{\mathrm{1r}}(m_1,1,m_2,1;\hat{m}_1,\hat{n}_1,\hat{m}_2,\hat{n}_2)}{2M_1M_2} \tag{11}$$

$$ABEP_{\hat{I}_1 \ne I_1, \hat{I}_2 = I_2} = \frac{\sum\limits_{m_1=1}^{M_1}\sum\limits_{m_2=1}^{M_2}\sum\limits_{\check{m}_1=1}^{M_1}\begin{bmatrix} D_{\mathrm{H}}(\check{m}_1,m_1)PEP_{\mathrm{1r}}(m_1,1,m_2,1;\check{m}_1,1,m_2,1) \\ +\left[\frac{N_1\log_2 N_1}{2}+(N_1-1)D_{\mathrm{H}}(\check{m}_1,m_1)\right]PEP_{\mathrm{1r}}(m_1,1,m_2,1;\check{m}_1,2,m_2,1)\end{bmatrix}}{M_1M_2\log_2(N_1M_1)} \tag{12}$$

$$ABEP_{\hat{I}_1 = I_1, \hat{I}_2 = I_2} = \frac{\sum\limits_{m_1=1}^{M_1}\sum\limits_{m_2=1}^{M_2}\sum\limits_{\check{m}_1=1}^{M_1}\begin{bmatrix} D_{\mathrm{H}}(\check{m}_1,m_1)PEP_{\mathrm{r2}}(m_1,1,m_2,1;\check{m}_1,1|m_2,1) \\ +\left[\frac{N_1\log_2 N_1}{2}+(N_1-1)D_{\mathrm{H}}(\check{m}_1,m_1)\right]PEP_{\mathrm{r2}}(m_1,1,m_2,1;\check{m}_1,2|m_2,1)\end{bmatrix}}{M_1M_2\log_2(N_1M_1)} \tag{13}$$

$$\upsilon = \begin{cases} \frac{\rho_1|x_1[m_1]-x_1[\hat{m}_1]|^2+\rho_2|x_2[m_2]-x_2[\hat{m}_2]|^2}{4\left(\rho_r^{1-\mu}|x_r[\hat{m}'_r]|^2+1\right)}, & \hat{n}_1=n_1, \hat{n}_2=n_2 \\ \frac{\rho_1|x_1[m_1]-x_1[\hat{m}_1]|^2+\rho_2\left(|x_2[m_2]|^2+|x_2[\hat{m}_2]|^2\right)}{4\left(\rho_r^{1-\mu}|x_r[\hat{m}'_r]|^2+1\right)}, & \hat{n}_1=n_1, \hat{n}_2\ne n_2 \\ \frac{\rho_1\left(|x_1[m_1]|^2+|x_1[\hat{m}_1]|^2\right)+\rho_2|x_2[m_2]-x_2[\hat{m}_2]|^2}{4\left(\rho_r^{1-\mu}|x_r[\hat{m}'_r]|^2+1\right)}, & \hat{n}_1\ne n_1, \hat{n}_2=n_2 \\ \frac{\rho_1\left(|x_1[m_1]|^2+|x_1[\hat{m}_1]|^2\right)+\rho_2\left(|x_2[m_2]|^2+|x_2[\hat{m}_2]|^2\right)}{4\left(\rho_r^{1-\mu}|x_r[\hat{m}'_r]|^2+1\right)}, & \hat{n}_1\ne n_1, \hat{n}_2\ne n_2 \end{cases} \tag{15}$$

$$\xi = \begin{cases} \frac{\rho_r|x_r[m_1+(m_2-1)M_1]-x_r[\check{m}_1+(m_2-1)M_1]|^2}{4(\rho_2^{1-\mu}|x_2[m'_2,k+1]|^2+1)}, & \check{n}_r = n_r \\ \frac{\rho_r(|x_r[m_1+(m_2-1)M_1]|^2+|x_r[\check{m}_1+(m_2-1)M_1]|^2)}{4(\rho_2^{1-\mu}|x_2[m'_2,k+1]|^2+1)}, & \check{n}_r \ne n_r \end{cases} \tag{17}$$

$$\mathbf{d}_{r2} \triangleq \sqrt{\rho_{\mathrm{e},r2}}\left\|\mathbf{h}_{r2}[k+1,1]\,x_r[k+1,m_1+(m_2-1)M_1] - \mathbf{h}_{r2}[k+1,\check{n}_1]\,x_r[k+1,\check{m}_1+(m_2-1)M_1]\right\|^2 \tag{18}$$

Proposition 2. *Assuming $\rho_r = \rho_i = \rho$, an asymptotic ABEP of FD-TWRC-SM is computed by (23), where G_1 and G_2 are respectively computed by Eqs. (24) and (25) with (26) and (27), $N_{\mathrm{R}} = \min\{N_{\mathrm{R,r}}, N_{\mathrm{R,2}}\}$, $\binom{N}{k_1,k_2,\ldots,k_m} \triangleq \frac{n!}{k_1!k_2!\ldots k_m!}$, and*

$$K_1(q) = \sum_{\hat{m}_r'=1}^{M_1M_2} \binom{2N_{\mathrm{R,r}}-1}{N_{\mathrm{R,r}}-1, N_{\mathrm{R,r}}-q, q} |x_r[\hat{m}_r']|^{2q}, \tag{28}$$

$$K_2(q) = \sum_{m_2'=1}^{M_2} \binom{2N_{\mathrm{R,2}}-1}{N_{\mathrm{R,2}}-1, N_{\mathrm{R,2}}-q, q} |x_2[m_2', k+1]|^{2q}. \tag{29}$$

Proof: See Appendix C. ■

Remark 1. *It is observed in (23) that the ABEP increases dramatically with the decreasing SI cancellation factor μ. From (23), we find that the ABEP is a weighted summation of $\rho^{-N_{\mathrm{R},r}+q(1-\mu)}$, $\rho^{-N_{\mathrm{R}}+q(1-\mu)}$, and $\rho^{-N_{\mathrm{R,2}}+q(1-\mu)}$ respectively when $N_{\mathrm{R,r}} < N_{\mathrm{R,2}}$, $N_{\mathrm{R,r}} = N_{\mathrm{R,2}}$, and $N_{\mathrm{R,r}} > N_{\mathrm{R,2}}$. In the high SNR regime, the worst term dominates the slope of the ABEP, which is defined as the diversity order [7, Proposition 4]. Thus, when $N_{\mathrm{R,r}} < N_{\mathrm{R,2}}$, the diversity order is $\min_q\{N_{\mathrm{R,2}} - q(1-\mu)\} = \mu N_{\mathrm{R,2}}$. Similarly, when $N_{\mathrm{R,r}} = N_{\mathrm{R,2}}$ and $N_{\mathrm{R,r}} > N_{\mathrm{R,2}}$, we have diversity orders μN_R and $\mu N_{R,r}$, respectively. Therefore, the diversity order of the FD-TWRC-SM system is $\min\{\mu N_{\mathrm{R},r}, \mu N_{\mathrm{R,2}}\}$. We take $N_{\mathrm{R},r} = 1$ and $N_{\mathrm{R,2}} = 2$ as an example, from the first line of (23), we obtain $ABEP_{\mathrm{FD,A}} = G_1[K_1(0)\rho^{-1} + K_1(1)\rho^{-\mu}] \doteq G_1K_1(1)\rho^{-\mu}$ and thus the diversity order is μ.*

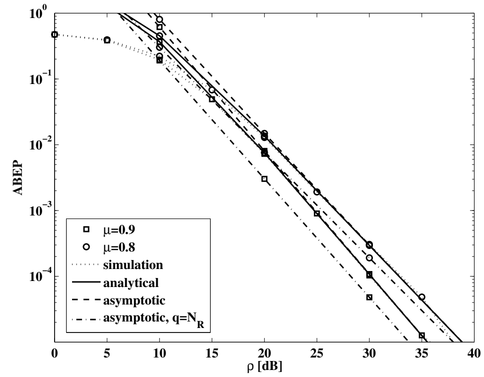

Fig. 3. Verification of Remark 1.

However, if we use $\lim_{\rho\to+\infty} G \sum_{q=0}^{N_{\mathrm{R}}} K(q)\rho^{-N_{\mathrm{R}}+q(1-\mu)} = GK(q)\rho^{-N_{\mathrm{R}}\mu}$ [7, Corollary 5] in (23) by letting $q = N_{\mathrm{R}}$, then the obtained asymptotic ABEP will not be tight enough to analyze the system performance because when μ is large, $\rho^{-(1-\mu)-\mu N_{\mathrm{R}}} << \rho^{-\mu N_{\mathrm{R}}}$ may not hold. Thus, we use (23)

$$\upsilon_{\mathrm{HD}} = \begin{cases} \frac{\rho_1|x_1[m_1]-x_1[\hat{m}_1]|^2+\rho_2|x_2[m_2]-x_2[\hat{m}_2]|^2}{4}, & \hat{n}_1 = n_1, \hat{n}_2 = n_2 \\ \frac{\rho_1|x_1[m_1]-x_1[\hat{m}_1]|^2+\rho_2\left(|x_2[m_2]|^2+|x_2[\hat{m}_2]|^2\right)}{4}, & \hat{n}_1 = n_1, \hat{n}_2 \neq n_2 \\ \frac{\rho_1\left(|x_1[m_1]|^2+|x_1[\hat{m}_1]|^2\right)+\rho_2|x_2[m_2]-x_2[\hat{m}_2]|^2}{4}, & \hat{n}_1 \neq n_1, \hat{n}_2 = n_2 \\ \frac{\rho_1\left(|x_1[m_1]|^2+|x_1[\hat{m}_1]|^2\right)+\rho_2\left(|x_2[m_2]|^2+|x_2[\hat{m}_2]|^2\right)}{4}, & \hat{n}_1 \neq n_1, \hat{n}_2 \neq n_2 \end{cases} \tag{21}$$

$$\xi_{\mathrm{HD}} = \begin{cases} \frac{\rho_r|x_r[m_1+(m_2-1)M_1]-x_r[\check{m}_1+(m_2-1)M_1]|^2}{4}, & \hat{n}_r = n_r \\ \frac{\rho_r(|x_r[m_1+(m_2-1)M_1]|^2+|x_r[\check{m}_1+(m_2-1)M_1]|^2)}{4}, & \hat{n}_r \neq n_r \end{cases} \tag{22}$$

$$ABEP_{\mathrm{FD,A}} = \begin{cases} G_1 \sum_{q=0}^{N_{\mathrm{R,r}}} K_1(q)\rho^{-N_{\mathrm{R,r}}+q(1-\mu)}, & N_{\mathrm{R,r}} < N_{\mathrm{R,2}} \\ \sum_{q=0}^{N_{\mathrm{R}}} (G_1K_1(q) + G_2K_2(q))\rho^{-N_{\mathrm{R}}+q(1-\mu)}, & N_{\mathrm{R,r}} = N_{\mathrm{R,2}} \\ G_2 \sum_{q=0}^{N_{\mathrm{R,2}}} K_2(q)\rho^{-N_{\mathrm{R,2}}+q(1-\mu)}, & N_{\mathrm{R,r}} > N_{\mathrm{R,2}} \end{cases} \tag{23}$$

$$G_1 = \frac{1}{M_1^2M_2^2} \sum_{m_1=1}^{M_1} \sum_{m_2=1}^{M_2} \left\{ \begin{array}{c} \sum_{\hat{I}_1=(1,1)}^{(M_1,N_1)} \sum_{\hat{I}_2 \neq I_2=(1,1)}^{(M_2,N_2)} \frac{1}{2\upsilon_0(m_1,1,m_2,1;\hat{m}_1,\hat{n}_1,\hat{m}_2,\hat{n}_2,\check{m}_1,\check{n}_1)^{N_{\mathrm{R,r}}}} \\ + \frac{\sum_{\check{m}_1=1}^{M_1}\left[\frac{D_{\mathrm{H}}(\check{m}_1,m_1)}{\upsilon_0(m_1,1,m_2,1;\check{m}_1,1,m_2,1)^{N_{\mathrm{R,r}}}} + \frac{\left[\frac{N_1\log_2 N_1}{2}+(N_1-1)D_{\mathrm{H}}(\check{m}_1,m_1)\right]}{\upsilon_0(m_1,1,m_2,1;\check{m}_1,2,m_2,1)^{N_{\mathrm{R,r}}}}\right]}{\log_2(N_1M_1)} \end{array} \right\}, \tag{24}$$

$$G_2 = \frac{\sum_{m_1=1}^{M_1}\sum_{m_2=1}^{M_2}\sum_{\check{m}_1=1}^{M_1}\left[\frac{D_{\mathrm{H}}(\check{m}_1,m_1)}{\xi_0(m_1,1,m_2,1;\check{m}_1,1|m_2,1)^{N_{R,2}}} + \frac{\left[\frac{N_1\log_2 N_1}{2}+(N_1-1)D_{\mathrm{H}}(\check{m}_1,m_1)\right]}{\xi_0(m_1,1,m_2,1;\check{m}_1,2|m_2,1)^{N_{R,2}}}\right]}{M_1M_2^2\log_2(N_1M_1)} \tag{25}$$

$$\upsilon_0 = \begin{cases} |x_1[m_1]-x_1[\hat{m}_1]|^2 + |x_2[m_2]-x_2[\hat{m}_2]|^2, & \hat{n}_1 = n_1, \hat{n}_2 = n_2 \\ |x_1[m_1]-x_1[\hat{m}_1]|^2 + |x_2[m_2]|^2 + |x_2[\hat{m}_2]|^2, & \hat{n}_1 = n_1, \hat{n}_2 \neq n_2 \\ |x_1[m_1]|^2 + |x_1[\hat{m}_1]|^2 + |x_2[m_2]-x_2[\hat{m}_2]|^2, & \hat{n}_1 \neq n_1, \hat{n}_2 = n_2 \\ |x_1[m_1]|^2 + |x_1[\hat{m}_1]|^2 + |x_2[m_2]|^2 + |x_2[\hat{m}_2]|^2, & \hat{n}_1 \neq n_1, \hat{n}_2 \neq n_2 \end{cases} \tag{26}$$

$$\xi_0 = \begin{cases} |x_r[m_1+(m_2-1)M_1] - x_r[\check{m}_1+(m_2-1)M_1]|^2, & \check{n}_r = \hat{n}_r \\ |x_r[m_1+(m_2-1)M_1]|^2 + |x_r[\check{m}_1+(m_2-1)M_1]|^2, & \check{n}_r \neq \hat{n}_r \end{cases} \tag{27}$$

as the asymptotic performance in the high SNR regime. A verification of this remark is shown in Fig. 3, where we use $N_1 = N_2 = 4$*,* $M_1 = M_2 = 4$*, and* $N_{\mathrm{R,r}} = N_{\mathrm{R,2}} = 2$.

B. Optimal selection between HD and FD modes

In this subsection, we give comparisons of FD-TWRC-SM with its HD counterpart. To this, we first give an asymptotic ABEP of HD-TWRC-SM, which is derived based on $PEP_{\mathrm{HD,1r}}$ and $PEP_{\mathrm{HD,r2}}$. Following the same steps as in Appendix C, using (10) and Lemma 3, we obtain an asymptotic ABEP of HD-TWRC-SM in Lemma 4.

Lemma 4. *Assuming an equal average SNR at the nodes, i.e.,* $\rho_r = \rho_i = \rho$*, an asymptotic ABEP of HD-TWRC-SM is computed as (30), where* G_1 *and* G_2 *are defined in (24) and (25), respectively.*

Remark 2. *Under the same data rate, the signal constellation order* M_i *of HD-TWRC-SM is higher than that of FD-TWRC-SM. Therefore, it is predictable that with perfect SI cancellation, although these two systems have the same diversity order* $\min\{N_{\mathrm{R},r}, N_{\mathrm{R},2}\}$*, the Euclidean distance between the symbols in HD-TWRC-SM is smaller than that in FD-TWRC-SM. Thus, FD-TWRC-SM always performs better than HD-TWRC-SM in terms of ABEP. On the other hand, in the presence of non-perfect SI cancellation, the diversity order of FD-TWRC-SM is smaller than that of HD-TWRC-SM. Thus, HD-TWRC-SM tends to perform better than FD-TWRC as the SNR increases. Thus, an interesting and challenging problem is to figure out the SNR threshold for the selection of either HD or FD mode, through which ABEPs can be minimized over the entire SNR regime. The main result is summarized in Proposition 3.*

Proposition 3. *Assuming an equal average SNR* $\rho_r = \rho_i = \rho$ *at the nodes, the optimal selection of either FD or HD transmission modes is determined by*

$$\rho \underset{\mathrm{FD}}{\overset{\mathrm{HD}}{\gtrless}} z^{\frac{1}{(1-\mu)\min\{N_{\mathrm{R},r}, N_{\mathrm{R},2}\}}}, \tag{31}$$

where z *is the positive real root of Eq. (32) and can be represented in a closed form when* $\min\{N_{\mathrm{R},r}, N_{\mathrm{R},2}\} \leq 5$*. If* $\min\{N_{\mathrm{R},r}, N_{\mathrm{R},2}\} > 5$*, the positive real root of Eq. (32) can be obtained by Newton-Raphson method [61].*

$$\sum_{q=0}^{\min\{N_{\mathrm{R},r}, N_{\mathrm{R},2}\}} c_q z^q = c_{\mathrm{HD}}, \tag{32}$$

where

$$c_{\mathrm{HD}} = \begin{cases} G_{1,\mathrm{HD}} C_{2N_{\mathrm{R}}-1}^{N_{\mathrm{R}}}, & N_{\mathrm{R,r}} < N_{\mathrm{R,2}}, \\ (G_{1,\mathrm{HD}} + G_{2,\mathrm{HD}}) C_{2N_{\mathrm{R}}-1}^{N_{\mathrm{R}}}, & N_{\mathrm{R,r}} = N_{\mathrm{R,2}}, \\ G_{2,\mathrm{HD}} C_{2N_{\mathrm{R}}-1}^{N_{\mathrm{R}}}, & N_{\mathrm{R,r}} > N_{\mathrm{R,2}}, \end{cases} \tag{33}$$

$$c_q = \begin{cases} G_{1,\mathrm{FD}} K_1(q), & N_{\mathrm{R,r}} < N_{\mathrm{R,2}}, \\ G_{1,\mathrm{FD}} K_1(q) + G_{2,\mathrm{FD}} K_2(q), & N_{\mathrm{R,r}} = N_{\mathrm{R,2}}, \\ G_{2,\mathrm{FD}} K_2(q) \rho^{q(1-\mu)}, & N_{\mathrm{R,r}} > N_{\mathrm{R,2}}. \end{cases} \tag{34}$$

Proof: Letting $ABEP_{\mathrm{FD,A}} = ABEP_{\mathrm{HD,A}}$, we have (35). Letting $z = \rho^{1-\mu}$, (35) can be rewritten as (32). Then ρ, which is the root of (35), can be obtained by (31). ■

C. Power allocation

In subsections IV-A and IV-B, we assumed an equal average SNR at the nodes. The PA may be applied to achieve a better ABEP performance, where S_i and R employ different sets of powers $\rho_i \sigma^2$ and $\rho_r \sigma^2$, accordingly. In this subsection, we aim to propose an optimal PA under a total transmit power constraint $\rho_{\mathrm{All}} \sigma^2$, i.e., $2\rho_i \sigma^2 + \rho_r \sigma^2 \leq \rho_{\mathrm{All}} \sigma^2$. Defining PA factor $F \triangleq \frac{\rho_r}{\rho_i}$, we have $\rho_i \leq \frac{\rho_{\mathrm{All}}}{2+F}$ and $\rho_r \leq \frac{F\rho_{\mathrm{All}}}{2+F}$. Substituting them into Eqs. (10)-(17) and following the steps of proving Proposition 2, we have the following asymptotic ABEP of FD-TWRC-SM with unequal average SNRs at the nodes.

Lemma 5. *When* $2\rho_i + \rho_r = \rho_{\mathrm{All}}$*, the asymptotic ABEP of FD-TWRC-SM systems is computed by*

$$ABEP_{\mathrm{FD,PA}} \leq ABEP_{\mathrm{1r,FD,PA}} + ABEP_{\mathrm{r2,FD,PA}}, \tag{36}$$

$ABEP_{\mathrm{1r,FD,PA}}$ *and* $ABEP_{\mathrm{r2,FD,PA}}$ *are respectively computed by (37) and (38), where*

$$\begin{aligned} L_1(F) &= \frac{F^{q_1(1-\mu)}}{(2+F)^{-N_{\mathrm{R},r}+q_1(1-\mu)}} \\ &= \left(\frac{F}{2+F}\right)^{q_1(1-\mu)} (2+F)^{N_{\mathrm{R},r}}, \end{aligned} \tag{39}$$

$$\begin{aligned} L_2(F) &= \frac{F^{-N_{\mathrm{R},2}}}{(2+F)^{-N_{\mathrm{R},2}+q_2(1-\mu)}} \\ &= \left(\frac{F}{2+F}\right)^{-N_{\mathrm{R},2}} (2+F)^{-q_2(1-\mu)}, \end{aligned} \tag{40}$$

G_1*,* G_2*,* K_1*, and* K_2 *are computed by (24), (25), (28), and (29), respectively.*

It is observed that the power allocation does not affect the diversity order of the system, which is expressed by Eqs. (37)

$$ABEP_{\mathrm{HD,A}} = \begin{cases} G_1 C_{2N_{\mathrm{R}}-1}^{N_{\mathrm{R}}} \rho^{-N_{\mathrm{R}}}, & N_{\mathrm{R,r}} < N_{\mathrm{R,2}} \\ (G_1 + G_2) C_{2N_{\mathrm{R}}-1}^{N_{\mathrm{R}}} \rho^{-N_{\mathrm{R}}}, & N_{\mathrm{R,r}} = N_{\mathrm{R,2}} \\ G_2 C_{2N_{\mathrm{R}}-1}^{N_{\mathrm{R}}} \rho^{-N_{\mathrm{R}}}, & N_{\mathrm{R}} > N_{\mathrm{R,2}} \end{cases} \tag{30}$$

$$\begin{cases} G_{1,\mathrm{HD}} C_{2N_{\mathrm{R}}-1}^{N_{\mathrm{R}}} = G_{1,\mathrm{FD}} \sum_{q=0}^{N_{\mathrm{R}}} K_1(q) \rho^{q(1-\mu)}, & N_{\mathrm{R,r}} < N_{\mathrm{R,2}} \\ (G_{1,\mathrm{HD}} + G_{2,\mathrm{HD}}) C_{2N_{\mathrm{R}}-1}^{N_{\mathrm{R}}} = \sum_{q=0}^{N_{\mathrm{R}}} (G_{1,\mathrm{FD}} K_1(q) + G_{2,\mathrm{FD}} K_2(q)) \rho^{q(1-\mu)}, & N_{\mathrm{R,r}} = N_{\mathrm{R,2}} \\ G_{2,\mathrm{HD}} C_{2N_{\mathrm{R}}-1}^{N_{\mathrm{R}}} = G_{2,\mathrm{FD}} \sum_{q=0}^{N_{\mathrm{R}}} K_2(q) \rho^{q(1-\mu)}, & N_{\mathrm{R,r}} > N_{\mathrm{R,2}} \end{cases} \tag{35}$$

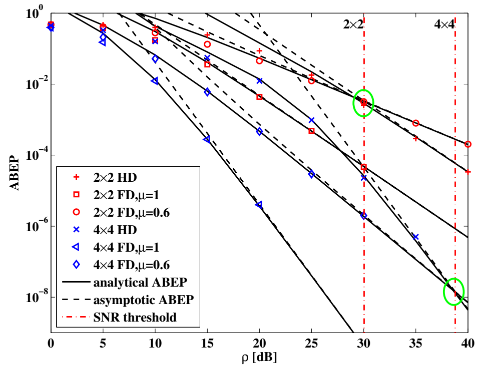

Fig. 4. Verification of the SNR threshold for the selection between HD/FD under 4bpcu TWRC-SM systems, where $\mu = 0.6$. Markers show Monte Carlo simulations based on 10^6 realizations, and solid lines and dashed lines show the analytical union-bounds. The SNR threshold is computed by (31).

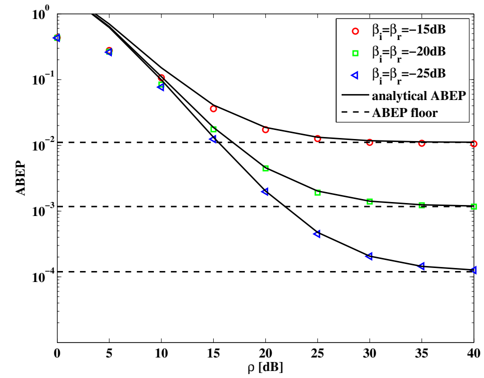

Fig. 5. Verification of the analytical upper bound on ABEP for 3bpcu TWRC-SM systems under constant interference model [51] where $N_{\mathrm{R},i} = N_{\mathrm{R},r} = 2$, $N_1 = N_2 = 4$ and $M_1 = M_2 = 2$. Markers show Monte Carlo simulations based on 10^6 realizations, and solid lines and dashed lines show the analytical union-bounds.

and (38), whereas the power allocation affects the coding gain. By using Lemma 5, an optimal PA factor is computed by Proposition 4.

Proposition 4. *The optimal PA factor is computed as follows.*

When $N_{\mathrm{R},r} = N_{\mathrm{R},2}$,

$$F = \sqrt[N_{\mathrm{R},2}+1]{A_{\mathrm{r}2} A_{1\mathrm{r}}^{-1}}, \tag{41}$$

where

$$A_{1\mathrm{r}} = N_{\mathrm{R},r} \sum_{q_1=0}^{N_{\mathrm{R,r}}} G_1 K_1(q_1) \rho_{\mathrm{All}}^{-N_{\mathrm{R},r}+q_1(1-\mu)}, \tag{42}$$

$$A_{\mathrm{r}2} = 2N_{\mathrm{R},2} \sum_{q_2=0}^{N_{\mathrm{R},2}} G_2 K_2(q_2) 2^{-q_2(1-\mu)} \rho_{\mathrm{All}}^{-N_{\mathrm{R},2}+q_2(1-\mu)}. \tag{43}$$

When $N_{\mathrm{R},r} > N_{\mathrm{R},2}$, the optimal F is the positive real root of Eq. (44), which can be represented in a closed form when $N_{\mathrm{R},r} \leq 4$. If $N_{\mathrm{R},r} > 4$, the positive real root of Eq. (44) can be obtained by Newton-Raphson method [61].

$$F^{N_{\mathrm{R},2}+1}(2+F)^{N_{\mathrm{R},r}-N_{\mathrm{R},2}} = A_{\mathrm{r}2} A_{1\mathrm{r}}^{-1}. \tag{44}$$

When $N_{\mathrm{R},r} < N_{\mathrm{R},2}$, the optimal F is the positive real root of Eq. (45), which can be represented in a closed form when $N_{\mathrm{R},2} \leq 4$. If $N_{\mathrm{R},2} > 4$, the positive real root of Eq. (45) can be obtained by Newton-Raphson method [61].

$$F^{N_{\mathrm{R},2}+1} = A_{\mathrm{r}2} A_{1\mathrm{r}}^{-1} (2+F)^{N_{\mathrm{R},2}-N_{\mathrm{R},r}}. \tag{45}$$

Proof: See Appendix D. ■

V. Numerical Results

A. Verification

The aim of this subsection is to substantiate the analytical results obtained in this paper through numerical results. Three case studies are considered: i) ABEP upper bounds over i.i.d. Rayleigh channels. ii) SNR threshold for the selection between HD and FD under the same spectrum efficiency. iii) Optimal PA factor under a given total ρ_{All}.

1) Verification of ABEP upper bounds and SNR threshold for HD/FD selection: In Fig. 4, for 3bpcu FD-TWRC-SM and HD-TWRC-SM systems the analytical upper bounds on the ABEP, Monte Carlo simulation results for 10^6 channel realizations, and the asymptotic ABEPs are plotted where $N_1 = N_2 = 4$ for both FD and HD systems and the average SNR is $\rho_i = \rho_r = \rho$. In FD-TWRC-SM, we use $M_1 = M_2 = 2$, whereas in HD-TWRC-SM we use $M_1 = M_2 = 16$. The analytical upper bounds on the ABEPs of FD-TWRC-SM are computed by (10) using (14) and (16), whereas the analytical upper bounds on the ABEPs of HD-TWRC-SM are computed by (10) using (19) and (20). The asymptotic ABEPs of FD-TWRC-SM are computed by (23), whereas the asymptotic ABEPs of HD-TWRC-SM are computed by (30). It is observed in Fig. 4 that as the SNR increases, the difference between the analytical upper bound on the ABEP and the exact ABEP becomes negligible.

Moreover, the analytical SNR threshold given in (31) is also plotted using dashed lines. It is observed that the proposed SNR threshold for the selection between FD/HD agrees well with the point of intersection between the asymptotic ABEPs of FD and HD systems. Then this SNR threshold (31) can be utilized to decide whether FD transmission or HD transmission should be adopted to enhance the performance of TWRC-SM systems.

In section II, we showed an alternative constant SIR model [51]. The ABEP of FD-TWRC-SM systems under a constant SIR model is plotted in Fig. 5. It is observed that under the constant SIR model, there exists an ABEP floor that decreases with an increasing SIR β as consistent with the result in [51].

$$ABEP_{1\mathrm{r,FD,PA}} \leq \sum_{q_1=0}^{N_{\mathrm{R,r}}} G_1 K_1(q_1) L_1(F) \rho_{\mathrm{All}}^{-N_{\mathrm{R},r}+q_1(1-\mu)} \tag{37}$$

$$ABEP_{\mathrm{r}2\mathrm{,FD,PA}} \leq \sum_{q_2=0}^{N_{\mathrm{R},2}} G_2 K_2(q_2) L_2(F) \rho_{\mathrm{All}}^{-N_{\mathrm{R},2}+q_2(1-\mu)} \tag{38}$$

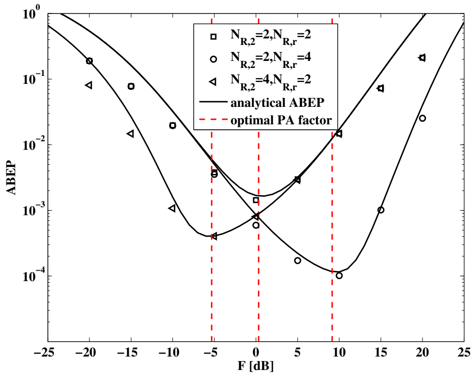

Fig. 6. Verification of the PA factor for FD-TWRC-SM systems where $\mu = 0.8$. Markers show Monte Carlo simulations based on 10^6 realizations, solid lines show the analytical union-bounds, and dashed lines show the optimal power allocation factor F.

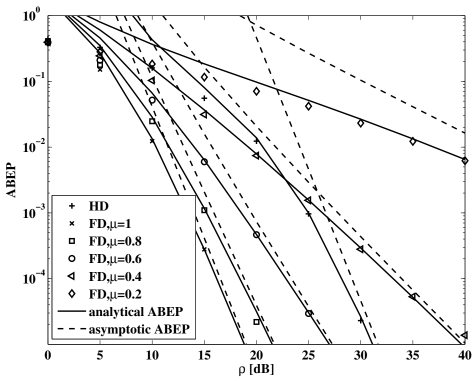

Fig. 7. Verification of the analytical upper bound and asymptotic ABEPs TWRC-SM systems. Markers show Monte Carlo simulations based on 10^6 realizations, and solid lines and dashed lines show the analytical union-bounds.

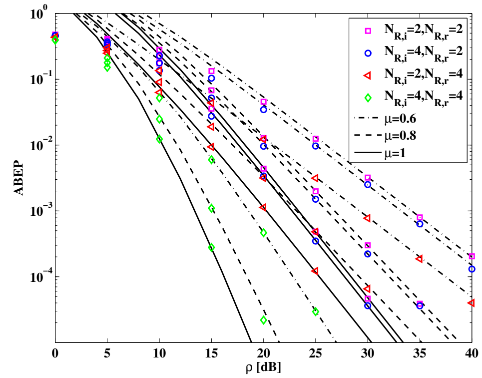

Fig. 8. The ABEP of FD-TWRC-SM for various sizes of the receive antenna array at 3bpcu data rate, where $M_i = 2$ and $N_i = 4$. Markers show Monte Carlo simulations based on 10^6 realizations, and solid lines and dashed lines show the analytical union-bounds.

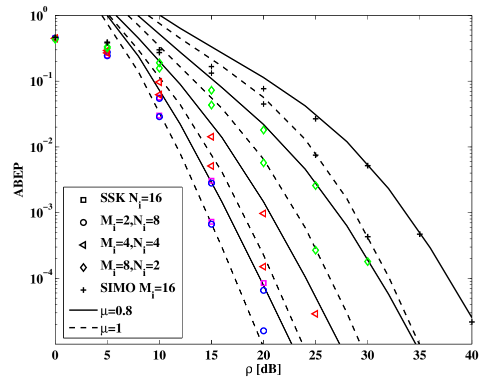

Fig. 9. The performance of FD-TWRC-SM for various sizes of signal and spatial constellation diagrams at 4bpcu data rate. Markers show Monte Carlo simulations based on 10^6 realizations, and solid lines and dashed lines show the analytical union-bounds.

2) Verification of optimal power allocation: The optimal PA factors computed by Proposition 4 and ABEP upper bounds of both FD and HD systems computed by (10)-(17) are given in Fig. 6, with 4bpcu data rate, $N_1 = N_2 = 4$ and $M_1 = M_2 = 4$. It is observed that the optimal PA factors F can minimize the ABEP of FD-TWRC-SM systems. It is observed that the best ABEP can be achieved at $F \approx 0$dB when $N_{\mathrm{R},2} = N_{\mathrm{R,r}}$. However, the best ABEP is achieved at $F < 0$dB or $F > 0$dB depending on the relationship between $N_{\mathrm{R},2}$ and $N_{\mathrm{R,r}}$.

B. System performance under various system parameters

First, we compare the ABEPs of FD-TWRC-SM systems under different μ in Fig. 7 with $N_{\mathrm{R},i} = N_{\mathrm{R},r} = 4$. In FD-TWRC-SM systems, we use $N_i = 4$ and $M_i = 2$, whereas $N_i = 4$ and $M_i = 16$ are used in HD-TWRC-SM systems. We find that a good SI cancellation is a prerequisite to employ FD transmissions in the TWRC-SM system and the diversity order is $\mu \min\{N_{R,i}, N_{R,r}\}$. When $\mu < 0.4$, the ABEP is higher than 10^{-5} even at a 40dB SNR, which is unacceptable in a realistic system, then the HD system will be a better choice than the FD system.

Then, we analyze the performance of FD-TWRC-SM for various system parameters. Especially, we investigate diversity properties of FD-TWRC-SM systems for various numbers of receive antennas. Also, we evaluate the ABEPs of FD-TWRC-SM systems and then compare them for different numbers of receive antennas at a given data rate constraint. Furthermore, we analyze the impact of an increasing number of transmit antennas on the ABEP at a given signal constellation diagram. Firstly, we investigate the impact of the number of receive antennas on the ABEP at a 3bpcu data rate in Fig. 8 with $M_1 = M_2 = 2$ and $N_1 = N_2 = 4$. It is observed that the ABEP decreases by increasing $N_{\mathrm{R,r}}$ and/or $N_{\mathrm{R},i}$. However, the system performance can not be improved significantly by solely increasing $N_{\mathrm{R,r}}$ or $N_{\mathrm{R},i}$. To improve the diversity performance of FD-TWRC-SM systems, we need to increase both $N_{\mathrm{R,r}}$ and $N_{\mathrm{R},i}$ simultaneously.

In 5G cellular networks, energy efficient massive MIMO will be employed, where hundreds of antennas are utilized for transmitting gigabit-level wireless traffic [57]. When $N_i > 16$, the number of transmit antennas at R is greater than 256, and the proposed FD-TWRC-SM system can be seen as a two-way FD massive MIMO. Since SM system is a promising candidate in low-complexity massive MIMO implementations [58], we investigate the impact of the increasing transmit antennas and evaluate the potential performance gains of FD-TWRC-SM systems. With a data rate constraint, the ABEPs against SNR are plotted in Fig. 9. We have the following observations.

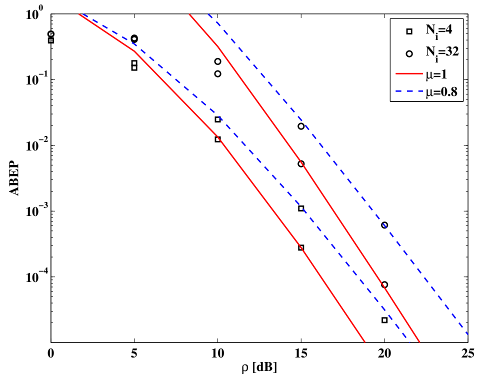

Fig. 10. The performance of FD-TWRC-SM for various sizes of spatial constellation diagrams at BPSK signal constellation diagram. Markers show Monte Carlo simulations based on 10^6 realizations, and solid lines and dashed lines show the analytical union-bounds.

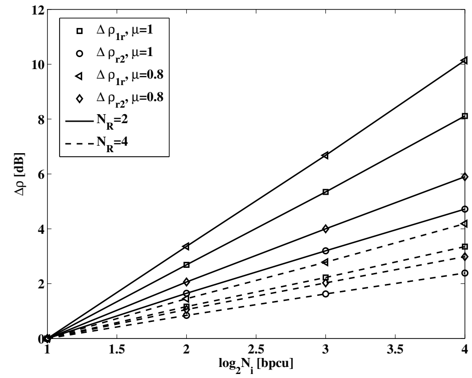

Fig. 11. Approximate SNR losses of both hops caused by adding transmit antennas for BPSK signal constellation.

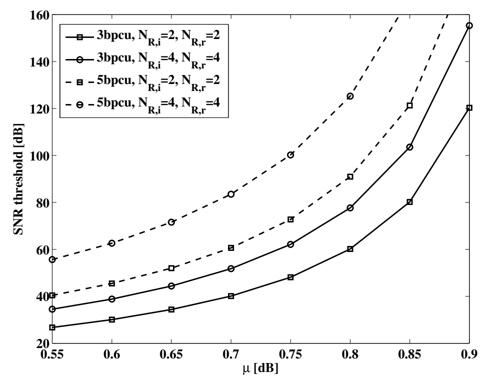

Fig. 12. The SNR threshold (31) for the selection between HD and FD with varying values of μ.

1) At a fixed data rate, the ABEP of FD-TWRC-SM systems decreases by increasing N_i. As a specific configuration of the FD-TWRC-SM system, the FD-TWRC-single input multiple output (SIMO) system, where $N_i = 1$, performs as the worst one under a given data rate.
2) The ABEP of FD-TWRC-SM systems with BPSK signal constellation diagram is nearly the same as FD-TWRC-SSK systems at the same data rate. Similar phenomenon can be found in single link SM transmissions [7, Figs. 9-10]. Considering both ABEP and the size of the transmit antenna array, BPSK can be seen as the optimal choice of signal constellation.

With $M_i = 2$, the ABEPs against SNR are plotted in Fig. 10 with $N_{\mathrm{R},r} = N_{\mathrm{R},i} = 4$. It is observed that with a given signal constellation diagram, the SNR loss, which is caused by increasing N_i, is quite small. According to (28), (29), (24), and (25), we can see that the number of transmit antennas N_i is irrelevant to K_1 and K_2 at a fixed M_i, whereas it impacts G_1 and G_2 simultaneously. Therefore, using $N_i = 2$ as a benchmark, the ABEP losses caused by increasing the transmit antennas of the first and the second hops are respectively computed by $\frac{ABEP_{1\mathrm{r}}}{ABEP_{1\mathrm{r},N_i=2}} = \frac{G_1}{G_{1,N_i=2}}$ and $\frac{ABEP_{\mathrm{r}2}}{ABEP_{\mathrm{r}2,N_i=2}} = \frac{G_2}{G_{2,N_i=2}}$. Since the diversity orders of both hops in FD-TWRC-SM systems are respectively $\mu N_{\mathrm{R},r}$ and $\mu N_{\mathrm{R},i}$, in the high SNR regime, we obtain approximate SNR losses of both hops caused by adding transmit antennas as $\Delta\rho_{1r} = (G_1/G_{1,N_i=1})^{\frac{1}{\mu N_{\mathrm{R},r}}}$ and $\Delta\rho_{r2} = (G_2/G_{2,N_i=1})^{\frac{1}{\mu N_{\mathrm{R},2}}}$ [2], which are plotted in Fig. 11. We obtain the following observations.

1) For BPSK signal constellation and $N_{\mathrm{R}} = 4$, the SNR loss is less than 4 dB in general when the data rate is increased by 3bpcu. When $N_{\mathrm{R}} = 2$, the SNR loss is less than 10 dB. Thus, in a massive MIMO system with a less number of receive antennas in comparison with the number of transmit antennas [58], a $\log_2 N_1$ multiplexing gain can be achieved at the cost of only a slightly higher transmit power.
2) It is found that $\Delta\rho_{1r} > \Delta\rho_{r2}$ and therefore adding more transmit antennas impacts the first hop more significantly than the second hop in terms of the ABEP. Therefore, when $N_{\mathrm{R},r} > N_{\mathrm{R},i}$, the SNR loss will be smaller than other cases.
3) The SNR loss increases with increasing μ. Therefore, when we use FD-TWRC-SM scheme in TWRC massive MIMO, a better SI cancellation will achieve a lower SNR loss.

C. Optimal selection between HD and FD modes

The SNR thresholds against μ are illustrated in Fig. 12. In the 3bpcu TWRC-SM systems, we use $N_1 = N_2 = 4$ and $M_1 = M_2 = 2$ for FD-TWRC-SM, and $N_1 = N_2 = 4$ and $M_1 = M_2 = 16$ for HD-TWRC-SM, respectively. In the 5bpcu TWRC-SM systems, we use $N_1 = N_2 = 16$ and $M_1 = M_2 = 2$ for FD-TWRC-SM, and $N_1 = N_2 = 16$ and $M_1 = M_2 = 64$ for HD-TWRC-SM, respectively. Then we have the following observations.

1) It is observed that with a greater μ, the FD node is subject to a lower residual SI. Since the SNR threshold becomes higher, it is more beneficial to select FD transmissions in both low and modest SNR regimes. In particular, when $\mu > 0.8$, the SNR threshold is greater

[2]Although the SNR loss computed by using diversity order is not precise, it allows us to get very simple analysis on the impact of adding transmit antennas on the ABEP.

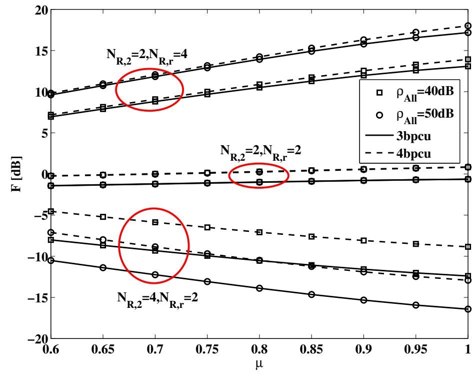

Fig. 13. The optimal PA factors F computed by Proposition 4 with varying values of μ.

than 60 dB, so that FD is always a better choice when $\rho \leq 60$ dB.

2) Under the same data rate constraint, we have $2\log_2 M_{\mathrm{FD},i} \ \ N_i = \log_2 M_{\mathrm{HD},i} \ \ N_i$, and therefore $M_{\mathrm{HD},i} = M_{\mathrm{FD},i}{}^2 N_i$. When N_i increases, $M_{\mathrm{HD},i}$ becomes so large that the Euclidean distance of adjacent signal symbols is very small and the performance of HD systems is deteriorated significantly. Specifically, when $N_i = 16$ and $M_{\mathrm{FD},i} = 2$, the signal constellation diagram at R of the HD systems is 4096-QAM. In this case, as long as $\mu > 0.55$, the threshold in 5bpcu is always greater than 40 dB. Thus, we can say that for a massive MIMO system, the FD-TWRC-SM almost always works better than its HD counterpart.
3) With a less number of receive antennas, it is more beneficial to select the FD transmissions due to a higher SNR threshold. Similar phenomenon can be observed in Fig. 4.

D. Optimal power allocation

The optimal PA factors against μ are illustrated in Fig. 13. In the 3bpcu TWRC-SM systems, we use $N_1 = N_2 = 4$ and $M_1 = M_2 = 2$. In the 4bpcu TWRC-SM systems, we use $N_1 = N_2 = 4$ and $M_1 = M_2 = 4$. Then, we have the following observations.

1) When $N_{\mathrm{R},r} > N_{\mathrm{R},i}$, F becomes large and greater than 5dB in general. The diversity order of the first hop is higher than that of the second hop, so that the ABEP of the second hop is the bottleneck of the overall ABEP. Therefore, we need to allocate more power to the second hop to obtain an optimal performance. Conversely, when $N_{\mathrm{R},r} < N_{\mathrm{R},i}$, we need to allocate more power to the first hop.
2) The optimal PA factor F increases with the data rate. The gap becomes more significant when $N_{\mathrm{R},r} < N_{\mathrm{R},i}$.
3) When $N_{\mathrm{R},r} = N_{\mathrm{R},i}$, the optimal PA factor F is independent of SNR. However, in other two cases, the total SNR should be taken into account carefully. For instance, the gap between Fs under 40dB and 50dB ρ_{ALL}s is about 3dB when $N_{\mathrm{R},r} \neq N_{\mathrm{R},i}$.
4) As μ increases, F behaves differently under different conditions. When $N_{\mathrm{R},r} = N_{\mathrm{R},i}$, F seems to be almost independent of μ. When $N_{\mathrm{R},r} > N_{\mathrm{R},i}$, F increases with an increasing μ. When $N_{\mathrm{R},r} < N_{\mathrm{R},i}$, F decreases with an increasing μ.

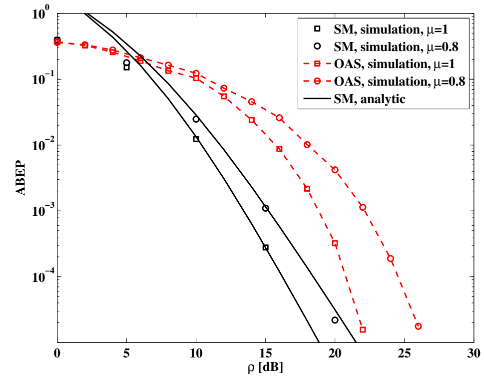

(a) 3bpcu

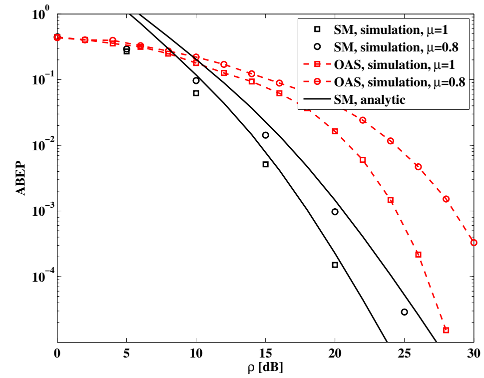

(b) 4bpcu

Fig. 14. ABEP comparison of the proposed FD-TWRC-SM system with the FD-TWRC-OAS system.

E. Comparison with single optimal antenna selection

As another category of MIMO systems with a single transmit RF chain, the optimal antenna selection (OAS) system has been widely investigated and introduced into TWRC transmission [56], [59]. In this section, we compare the performance of the proposed FD-TWRC-SM system with that of the FD-TWRC-OAS system. In the FD-TWRC-OAS system, optimal transmit antennas in term of the received signal strength of the intended signal are selected to transmit QAM signals in the first hop and the max-min antenna selection algorithm proposed in [56, Algorithm 1] is employed in the second hop. For sake of fair comparisons, the transmission rule of FD-TWRC-OAS is identical with that of the proposed FD-TWRC-SM system. In [56], S_is transmit their respective signals to R in two time blocks successively, whereas in the considered FD-TWRC-OAS system in this subsection, both S_is transmit signals to R simultaneously in a single time block, as consistent with Fig. 2.

The ABEP comparison of the proposed FD-TWRC-SM system with the FD-TWRC-OAS system are plotted in Fig. 14 where $N_{R,i} = N_{R,r} = 4$. Since it is intractable to analytically derive the ABEP of the FD-TWRC-OAS system due to the complex distribution of the channel amplitude after transmit antenna selection and the superposition of two independent signals from both sources, we plot the ABEP of the FD-TWRC-OAS system by using Monte Carlo simulations. Under 3bpcu configuration, we use $M_i = 2$, $N_i = 4$ for the FD-TWRC-SM system, and $M_i = 8$, $N_i = 4$ for the FD-TWRC-OAS system. Whereas under 4bpcu configuration, we use $M_i = 4$, $N_i = 4$ for the FD-TWRC-SM system, and $M_i = 16$, $N_i = 4$ for the FD-TWRC-OAS system. In the OAS system, both the transmitter and the receiver need to know the CSI, but in the SM system, the CSI is only required by the receiver. It is found in Fig. 14 that the FD-TWRC-OAS system has a higher diversity order than the FD-TWRC-SM system. Nevertheless, under typical configurations, the FD-TWRC-SM performs better than the FD-TWRC-OAS system because the information that is mapped onto the spatial constellation can efficiently reduce the size of the signal constellation.

VI. Conclusions

In this paper, we have proposed a FD-TWRC-SM with the optimal ML detector employed at each node. Firstly, a tight ABEP upper bound of the referred system has been derived in the closed form expression under i.i.d. Rayleigh fading channels. From the analytical ABEP analysis, we have found that the diversity order of the FD-TWRC-SM system is determined by the quality of SI cancellation. Then, we have conducted an extensive simulation campaign to evaluate the system performance. We have found that the proposed FD-TWRC-SM system is a promising candidate in low-complexity TWRC massive MIMO implementations because of its low SNR loss caused by multiplexing gain that is provided by adding transmit antennas. In addition, both HD-TWRC-SM and FD-TWRC-SM systems have been compared in terms of the ABEP. The exact SNR threshold, below which a better performance can be achieved by FD-TWRC-SM over HD-TWRC-SM, is analytically derived in a closed form. It has been observed that the FD-TWRC-SM with a reasonably good SI cancellation works better than its HD counterpart. Moreover, we have investigated the power allocation among sources and relay by deriving the optimal PA factor in a closed form. We have found that when $N_{\mathrm{R},r} > N_{\mathrm{R},i}$, more power needs to be allocated to the second hop to achieve an optimal performance. Whereas when $N_{\mathrm{R},r} < N_{\mathrm{R},i}$, more power needs to be allocated to the first hop. Finally, the SM system has been compared with the OAS system in FD-TWRC scheme. We have found that under typical configurations, the FD-TWRC-SM outperforms the FD-TWRC-OAS because the information that is mapped onto spatial constellation can efficiently reduce the size of the signal constellation.

However, since there is no any research on the modeling of the residual SI in the SM context, we will investigate the practical SI cancellation schemes in our future works. Some other SM systems will be incorporated into the FD-TWRC scheme, e.g., coded SM and generalised SM schemes. We will also investigate other types of arbitrary configurations with $N_r \neq N_1 N_2$, and $M_2 \neq M_1 M_2$. Moreover, we will investigate on derivation of a closed form ABEP of the FD-TWRC-OAS system.

Appendix

A. Proof of Proposition 1

Firstly, with i.i.d. channels, the ABEP is irrelevant to the specific antennas that are chosen to transmit signals at S_i. Without loss of generality, letting $n_1 = n_2 = 1$, (9) can be rewritten as (46). In the high SNR regime, the ABEP of the transmission is determined by the hop having a worse performance [56]. Therefore, two cases of error are considered, i.e., the errors that occur in the first and second hops. When the error occurs in the first hop, two cases have to be taken into account. First, I_2 is wrongly detected and therefore I_1 is not a candidate of the detection in the second hop. Second, I_2 is rightly detected while I_1 is a candidate of the detection in the second hop. Therefore, a detection error of I_1 might occur when i) I_2 is wrongly detected in the first hop; ii) I_2 is correctly detected but I_1 is wrongly detected in the first hop; or iii) both I_1 and I_2 are correctly detected in the first hop but I_1 is wrongly detected in the second hop. Then (46) is rewritten as (47).

$$ABEP \leq \frac{\sum_{m_1=1}^{M_1} \sum_{m_2=1}^{M_2} \sum_{\hat{I}_1=(1,1)}^{(M_1,N_1)} \sum_{\hat{I}_2=(1,1)}^{(M_2,N_2)} \sum_{\check{I}_1=(1,1)}^{(M_1,N_1)} D_{\mathrm{H}}\left(\check{n}_1, \check{m}_1, n_1, m_1\right) PEP\left(m_1, 1, m_2, 1, \hat{m}_1, \hat{n}_1, \hat{m}_2, \hat{n}_2, \check{m}_1, \check{n}_1\right)}{M_1 M_2 \log_2(N_1 M_1)} \tag{46}$$

$$\begin{aligned} ABEP \leq \sum_{m_1=1}^{M_1} \sum_{m_2=1}^{M_2} \Bigg[& \underbrace{\frac{\sum_{\hat{I}_1=(1,1)}^{(M_1,N_1)} \sum_{\hat{I}_2 \neq I_2=(1,1)}^{(M_2,N_2)} \sum_{\check{I}_1=(1,1)}^{(M_1,N_1)} D_{\mathrm{H}}(\check{n}_1,\check{m}_1,n_1,m_1) PEP(m_1,1,m_2,1,\hat{m}_1,\hat{n}_1,\hat{m}_2,\hat{n}_2,\check{m}_1,\check{n}_1)}{M_1 M_2 \log_2(N_1 M_1)}}_{ABEP_{\hat{I}_2 \neq I_2}} \\ & + \underbrace{\frac{\sum_{\hat{I}_1 \neq (m_1,1)=(1,1)}^{(M_1,N_1)} \sum_{\check{I}_1=(1,1)}^{(M_1,N_1)} D_{\mathrm{H}}(\check{n}_1,\check{m}_1,n_1,m_1) PEP(m_1,1,m_2,1,\hat{m}_1,\hat{n}_1,m_2,n_2,\check{m}_1,\check{n}_1)}{M_1 M_2 \log_2(N_1 M_1)}}_{ABEP_{\hat{I}_1 \neq I_1, \hat{I}_2 = I_2}} \\ & + \underbrace{\frac{\sum_{\check{I}_1=(1,1)}^{(M_1,N_1)} D_{\mathrm{H}}(\check{n}_1,\check{m}_1,n_1,m_1) PEP(m_1,1,m_2,1,m_1,1,m_2,1,\check{m}_1,\check{n}_1)}{M_1 M_2 \log_2(N_1 M_1)} \Bigg]}_{ABEP_{\hat{I}_1 = I_1, \hat{I}_2 = I_2}} \end{aligned} \tag{47}$$

Further simplification of $ABEP_{\hat{I}_2 \neq I_2}$, $ABEP_{\hat{I}_1 \neq I_1, \hat{I}_2 = I_2}$ and $ABEP_{\hat{I}_1 = I_1, \hat{I}_2 = I_2}$ can be obtained as follows:

1) When I_2 is wrongly detected by R in the first hop, i.e., $\hat{I}_2 \neq I_2$, according to (6), we have (48).
Even if the SI and noise can be neglected, i.e., $\sqrt{\rho_2^{1-\mu}}\mathbf{h}_{22}[k+1, n_2']x_2[m_2'] + \mathbf{w}_2[k+1] = 0$, there is no way to guarantee $\mathbf{h}_{r2}[k+1, \hat{n}_1 + (\hat{n}_2 - 1)N_1] = \mathbf{h}_{r2}[k+1, \check{n}_1 + (n_2 - 1)N_1]$ and $x_r[k+1, \hat{m}_1 + (\hat{m}_2 - 1)M_1] = x_r[k+1, \check{m}_1 + (m_2 - 1)M_1]$ for arbitrary I_1 and $\check{I}_1$. Therefore the oringinal I_1 is not a candidate while detecting $\check{I}_1$ at S_2 in the second hop and it is highly probable that $\check{I}_1 \neq I_1$. In this case, the union upper bound principle does no hold and the exact ABEP while $\hat{I}_2 \neq I_2$ is very difficult to derive. In this work, $\check{I}_1$ is seen as a random choice in all candidate I_1, and therefore as long as $\hat{I}_2 \neq I_2$, the conditional ABEP is set to 0.5, i.e., $ABEP_{\hat{I}_2 \neq I_2} = 0.5 \times \Pr(\hat{I}_2 \neq I_2)$ [3]. Thus we can obtain (11).
2) Similarly, the detection error $\hat{I}_1 \neq I_1, \hat{I}_2 = I_2$ occurs in the first hop and $ABEP_{\hat{I}_1 \neq I_1, \hat{I}_2 = I_2}$ is computed by (49). In the high SNR regime, if $\hat{I}_2$ is correctly detected at R and $\hat{I}_1$ is wrongly detected, then there exists a very high probability that $\check{I}_1$ is miss-detected as $\hat{I}_1$, i.e.,

$$\begin{aligned} &\lim_{\rho\to\infty} PEP_{\mathrm{r2}}\left(\hat{m}_1, \hat{n}_1, m_2, 1; \check{m}_1, \check{n}_1 | m_2, 1\right) \\ &\qquad = \delta\big(\hat{I}_1 - \check{I}_1\big). \end{aligned} \tag{50}$$

By substituting (50) into (49) and using some simple algebraic manipulations, we obtain (51). For any bit mapping, $D_{\mathrm{H}}\left(\check{m}_1, \check{n}_1, m_1, n_1\right) = D_{\mathrm{H}}\left(\hat{n}_1, n_1\right) + D_{\mathrm{H}}\left(\hat{m}_1, m_1\right)$. Therefore, when $\check{n}_1 = 1$, $D_{\mathrm{H}}\left(\check{n}_1, \check{m}_1, 1, m_1\right) = D_{\mathrm{H}}\left(\check{m}_1, m_1\right)$. When $\check{n}_1 \neq 1$, because $\sum\limits_{n_1=1}^{N_1} \sum\limits_{\hat{n}_1=1}^{N_1} D_{\mathrm{H}}\left(\hat{n}_1, n_1\right) = \frac{N_1^2}{2} \log_2 N_1$ [7, Corollary 1], we have $D_{\mathrm{H}}\left(\check{n}_1, \check{m}_1, 1, m_1\right) = \frac{N_1 \log_2 N_1}{2(N_1 - 1)} + D_{\mathrm{H}}\left(\check{m}_1, m_1\right)$. Similarly, with i.i.d. channels, the Euclidean distance of any pair of channel coefficients is the same on average. Thus (12) can be readily obtained after some algebraic manipulations.
3) When both I_1 and I_2 are correctly detected at R in the first hop, i.e., $\hat{I}_1 = I_1, \hat{I}_2 = I_2$, the detection error occurs only in the second hop, for which we have (52), and $ABEP_{\hat{I}_1 = I_1, \hat{I}_2 = I_2}$ is upper bounded as (53). Likewise, (13) can be obtained.

[3]The assumption of random choice is an approximation. It will be shown in Section V-A that the analytical results match the simulations very well, which validates this approximation.

B. Proof of Lemma 1

The residual SI and the noise are both complex Gaussian distributed with variances of $\rho_r^{1-\mu}$ and 1, respectively. If $(m_1, n_1, m_2, n_2) \neq (\hat{m}_1, \hat{n}_1, \hat{m}_2, \hat{n}_2)$, from (1), the transmission from S_i to R is equivalent to the SM transmission with an average SNR of $\rho_{\mathrm{e},i} = \frac{\rho_i}{\rho_r^{1-\mu}|x_r[\hat{m}_r']|^2 + 1}$. According to (5) and following the steps provided in [8, Section IV], PEP_{1r} between (m_1, n_1, m_2, n_2) and $(\hat{m}_1, \hat{n}_1, \hat{m}_2, \hat{n}_2)$ under given $\mathbf{h}_{1r}$ and $\mathbf{h}_{2r}$ is computed by

$$PEP_{1\mathrm{r}, \mathbf{h}_{1r}, \mathbf{h}_{2r}, \hat{m}_r'} = Q\left(\sqrt{d_{1r}/2}\right), \tag{54}$$

where d_{1r} is defined as (55). Since the elements of $\mathbf{h}_{1r}$ and $\mathbf{h}_{2r}$ are all complex Gaussian distributed and d_{1r} is a weighted sum of the norms of $\mathbf{h}_{1r}$ and $\mathbf{h}_{2r}$, the elements of $\sqrt{\rho_{\mathrm{e},1}}\mathbf{h}_{1r}[k, n_1]x_1[m_1] + \sqrt{\rho_{\mathrm{e},2}}\mathbf{h}_{2r}[k, n_2]x_2[m_2] - \sqrt{\rho_{\mathrm{e},1}}\mathbf{h}_{1r}[k, \hat{n}_1]x_1[\hat{m}_1] - \sqrt{\rho_{\mathrm{e},2}}\mathbf{h}_{2r}[k, \hat{n}_2]x_2[\hat{m}_2]$ are also complex Gaussian distributed. It is observed that the variance of $\sqrt{\rho_{\mathrm{e},1}}\mathbf{h}_{1r}[k, n_1]x_1[m_1] - \sqrt{\rho_{\mathrm{e},1}}\mathbf{h}_{1r}[k, \hat{n}_1]x_1[\hat{m}_1]$ depends on whether $\hat{n}_1$ is equal to n_1 or not. To be specific, if $\hat{n}_1 = n_1$, we have (56). Else if $\hat{n}_1 \neq n_1$, we have (57), where $\mathrm{D}[\cdot]$ denotes the variance. Similar discussion is applied to $\mathrm{D}\left[\sqrt{\rho_{\mathrm{e},2}}\mathbf{h}_{2r}[k, n_2]x_2[m_2] - \sqrt{\rho_{\mathrm{e},2}}\mathbf{h}_{2r}[k, \hat{n}_2]x_2[\hat{m}_2]\right]$.

Since the real part and imaginary part of $\mathbf{h}_{1r}$ and $\mathbf{h}_{2r}$ are all Gaussian distributed with a variance of 0.5, d_{1r} follows Chi-square distribution with a freedom degree of $2N_{\mathrm{R},r}$, i.e., $\frac{d_{1r}}{\sqrt{2\upsilon}} \sim \chi^2_{2N_{R,r}}$, where υ is defined in (15). Following the steps of [60, Eqs. (61)-(65)], we have

$$PEP_{1r, \hat{m}_r'} = \mathrm{E}_{\hat{m}_r'}\left[PEP_{1\mathrm{r}, \mathbf{h}_{1r}, \mathbf{h}_{2r}}\right] = \mathcal{R}(N_{\mathrm{R},r}, \upsilon), \tag{58}$$

based on which (14) can be obtained.

$$(\check{m}_1, \check{n}_1) = \mathop{\arg\min}_{\{\check{n}_1, \check{m}_1\}} \left\{ \left\| \begin{array}{c} \sqrt{\rho_r}\mathbf{h}_{r2}[k+1, \hat{n}_1 + (\hat{n}_2 - 1)N_1]x_r[k+1, \hat{m}_1 + (\hat{m}_2 - 1)M_1] \\ + \sqrt{\rho_2^{1-\mu}}\mathbf{h}_{22}[k+1, n_2']x_2[m_2'] + \mathbf{w}_2[k+1] \\ - \sqrt{\rho_r}\mathbf{h}_{r2}[k+1, \check{n}_1 + (n_2 - 1)N_1]x_r[k+1, \check{m}_1 + (m_2 - 1)M_1] \end{array} \right\| \right\} \tag{48}$$

$$\begin{aligned} ABEP_{\hat{I}_1 \neq I_1, \hat{I}_2 = I_2} = &\frac{\sum\limits_{m_1=1}^{M_1} \sum\limits_{m_2=1}^{M_2} \sum\limits_{\hat{I}_1 \neq (m_1, 1) = (1,1)}^{(M_1, N_1)} \sum\limits_{\check{I}_1 = (1,1)}^{(M_1, N_1)} D_{\mathrm{H}}(\check{n}_1, \check{m}_1, n_1, m_1)}{M_1 M_2 \log_2(N_1 M_1)} \\ &\times PEP_{1\mathrm{r}}\left(m_1, 1, m_2, 1; \hat{m}_1, \hat{n}_1, m_2, n_2\right) PEP_{\mathrm{r2}}\left(\hat{m}_1, \hat{n}_1, m_2, 1; \check{m}_1, \check{n}_1 | m_2, 1\right) \end{aligned} \tag{49}$$

$$ABEP_{\hat{I}_1 \neq I_1, \hat{I}_2 = I_2} = \frac{\sum\limits_{m_1=1}^{M_1} \sum\limits_{m_2=1}^{M_2} \sum\limits_{\check{I}_1 = (1,1)}^{(M_1, N_1)} D_{\mathrm{H}}\left(\check{n}_1, \check{m}_1, n_1, m_1\right) PEP_{1\mathrm{r}}\left(m_1, 1, m_2, 1; \check{m}_1, \check{n}_1, m_2, n_2\right)}{M_1 M_2 \log_2(N_1 M_1)} \tag{51}$$

$$PEP_{1\mathrm{r}}(m_1, 1, m_2, 1; \hat{m}_1, \hat{n}_1, \hat{m}_2, \hat{n}_2) = \delta(\hat{I}_1 - I_1) \times \delta(\hat{I}_2 - I_2) \tag{52}$$

$$ABEP_{\hat{I}_1 = I_1, \hat{I}_2 = I_2} \leq \frac{\sum\limits_{m_1=1}^{M_1} \sum\limits_{m_2=1}^{M_2} \sum\limits_{\check{I}_1 = (1,1)}^{(M_1, N_1)} D_{\mathrm{H}}\left(\check{n}_1, \check{m}_1, n_1, m_1\right) PEP_{\mathrm{r2}}\left(m_1, 1, m_2, 1; \check{m}_1, \check{n}_1 | m_2, 1\right)}{M_1 M_2 \log_2(N_1 M_1)} \tag{53}$$

C. Proof of Proposition 2

Using $\mathcal{R}(N_{\mathrm{R}},\kappa) \doteq 4^{-N_{\mathrm{R}}} C_{2N_{\mathrm{R}}-1}^{N_{\mathrm{R}}} \kappa^{-N_{\mathrm{R}}}$ [7, Corollary 5] and some algebraic manipulations of (14) and (16), the asymptotic $PEP_{1\mathrm{r,A}}$ and $PEP_{\mathrm{r2,A}}$ can be obtained as

$$PEP_{\mathrm{FD,1r,A}} \doteq \frac{\sum_{q=0}^{N_{\mathrm{R,r}}} K_1(q)\rho^{-N_{\mathrm{R,r}}+q(1-\mu)}}{M_1 M_2 {\upsilon_0}^{N_{\mathrm{R,r}}}}, \tag{59}$$

$$PEP_{\mathrm{FD,r2,A}} \doteq \frac{\sum_{q=0}^{N_{\mathrm{R,2}}} K_2(q)\rho^{-N_{\mathrm{R,2}}+q(1-\mu)}}{M_i {\xi_0}^{N_{\mathrm{R,2}}}}, \tag{60}$$

where $K_1(q)$, $K_2(q)$, υ_0, and ξ_0 are defined in (28), (29), (26), and (27), respectively. We define a notation $\doteq$ such that for a probability P, if $\lim\limits_{\rho\to+\infty} \frac{\log P}{\log \gamma\rho^{-\alpha}} = 1$, then we have $P \doteq \gamma\rho^{-\alpha}$ [42].

Substituting (59) and (60) into (11)-(13), we obtain the asymptotic union upper bound of $ABEP_{\hat{I}_2\neq I_2} + ABEP_{\hat{I}_1\neq I_1,\hat{I}_2=I_2}$, and $ABEP_{\hat{I}_1=I_1,\hat{I}_2=I_2}$ respectively as

$$\begin{aligned} &ABEP_{\hat{I}_2\neq I_2} + ABEP_{\hat{I}_1\neq I_1,\hat{I}_2=I_2} \\ &\qquad = G_1 \sum_{q=0}^{N_{\mathrm{R,r}}} K_1(q)\rho^{-N_{\mathrm{R,r}}+q(1-\mu)}, \end{aligned} \tag{61}$$

and

$$ABEP_{\hat{I}_1=I_1,\hat{I}_2=I_2} = G_2 \sum_{q=0}^{N_{\mathrm{R,2}}} K_2(q)\rho^{-N_{\mathrm{R,2}}+q(1-\mu)}. \tag{62}$$

For any given μ, we have (63). Thus, (23) is obtained and Proposition 2 is proved.

D. Proof of Proposition 4

To prove this proposition, we need to solve the equation $\frac{\partial ABEP_{\mathrm{FD,PA}}}{\partial F} = 0$. However, the optimal PA factor is difficult to derived in a closed form based on (37) and (38). In order to derive the optimal power allocation factor F, the following upper bound on $L_1(F)$ and $L_2(F)$ are employed.

$$L_1(F) \le (2+F)^{N_{\mathrm{R},r}}, \tag{64}$$

$$L_2(F) \le \left(\tfrac{F}{2+F}\right)^{-N_{\mathrm{R,2}}} 2^{-q_2(1-\mu)}. \tag{65}$$

In (64), the upper bound of $L_1(f)$ is given as the maximum sum quantity of the SNRs. Whereas in (65), if we also use the maximum sum quantity of the SNRs, we have $L_2(F) \le \left(\tfrac{F}{2+F}\right)^{-N_{\mathrm{R,2}}}$. Since, $L_2(F) \le \left(\tfrac{F}{2+F}\right)^{-N_{\mathrm{R,2}}} 2^{-q_2(1-\mu)} \le \left(\tfrac{F}{2+F}\right)^{-N_{\mathrm{R,2}}}$, $\left(\tfrac{F}{2+F}\right)^{-N_{\mathrm{R,2}}} 2^{-q_2(1-\mu)}$ is a tighter upper bound than $\left(\tfrac{F}{2+F}\right)^{-N_{\mathrm{R,2}}}$. In the following, the optimal PA factor is analyzed based on (65). Substituting Eqs. (64) and (65) respectively into Eqs. (37) and (38), we obtain (66) and (67). Since our target is to minimize $ABEP_{\mathrm{1r,FD,PA}} + ABEP_{\mathrm{r2,FD,PA}}$, we have (68), where A_{1r} and A_{r2} are computed by (42) and (43), respectively. Some simple algebraic manipulations lead to

$$F^{N_{\mathrm{R,2}}+1}(2+F)^{N_{\mathrm{R},r}-N_{\mathrm{R,2}}} = A_{\mathrm{r2}} A_{\mathrm{1r}}^{-1}, \tag{69}$$

and then we can obtain (41)-(45) by typical approaches for solving the polynomial equations.

REFERENCES

[1] X. Ge, et al., “Spatial Spectrum and Energy Efficiency of Random Cellular Networks,” *IEEE Trans. Commun.*, vol. 63, no. 3, pp. 1019 - 1030, 2015.

[2] R. Y. Mesleh, et al., “Spatial modulation,” *IEEE Trans. Veh. Technol.*, vol. 57, no. 4, pp. 2228-2242, 2008.

[3] M. Di Renzo, et al., “Spatial modulation for multiple-antenna wireless systems: a survey,” *IEEE Commun. Magazine,* vol. 49 , no.12, pp, 182-191, 2011.

[4] P. Yang, et al., “Design guidelines for spatial modulation,” *IEEE Commun. Surveys Tuts.*, vol. 17, no. 1, pp. 6-26, 2015.

[5] P. Yang, et al., “Single-carrier SM-MIMO: a promising design for broadband large-scale antenna systems,” *IEEE Commun. Surveys Tuts.*, to appear

[6] M. Di Renzo, et al., “Spatial modulation for generalized MIMO: challenges, opportunities, and implementation,” *IEEE Proc.*, vol. 102, no. 1, pp. 56-103, 2014.

[7] M. Di Renzo and H. Haas, “Bit error probability of SM-MIMO over generalized fading channels.” *IEEE Trans. Vehicular Tech.*, vol. 61, no. 3, pp. 1124-1144, 2012.

[8] J. Jeganathan, et al., “Spatial modulation: optimal detection and performance analysis,” *IEEE Commun. Lett.*, vol. 12, no. 8, pp. 545-547, 2008.

[9] E. Basar, et al., “Performance of spatial modulation in the presence of channel estimation errors,” *IEEE Commun. Lett.*, vol. 16, no. 2, pp. 176-179, 2012.

[10] M. Di Renzo and H. Haas, “Performance comparison of different spatial modulation schemes in correlated fading channels,” in Proc. *IEEE ICC*, pp. 1-6, 2010.

$$d_{1r} \triangleq \left\| \sqrt{\rho_{\mathrm{e},1}}\mathbf{h}_{1r}[k,n_1]x_1[m_1] + \sqrt{\rho_{\mathrm{e},2}}\mathbf{h}_{2r}[k,n_2]x_2[m_2] - \sqrt{\rho_{\mathrm{e},1}}\mathbf{h}_{1r}[k,\hat{n}_1]x_1[\hat{m}_1] - \sqrt{\rho_{\mathrm{e},2}}\mathbf{h}_{2r}[k,\hat{n}_2]x_2[\hat{m}_2] \right\|^2 \tag{55}$$

$$\mathrm{D}[\sqrt{\rho_{\mathrm{e},1}}\mathbf{h}_{1r}[k,n_1]x_1[m_1] - \sqrt{\rho_{\mathrm{e},1}}\mathbf{h}_{1r}[k,\hat{n}_1]x_1[\hat{m}_1]] = \rho_{\mathrm{e},1}|x_1[m_1] - x_1[\hat{m}_1]|^2 \tag{56}$$

$$\mathrm{D}[\sqrt{\rho_{\mathrm{e},1}}\mathbf{h}_{1r}[k,n_1]x_1[m_1] - \sqrt{\rho_{\mathrm{e},1}}\mathbf{h}_{1r}[k,\hat{n}_1]x_1[\hat{m}_1]] = \rho_{\mathrm{e},1}|x_1[m_1]|^2 + |x_1[\hat{m}_1]|^2 \tag{57}$$

$$G_1\rho^{-\mu N_1} + G_2\rho^{-\mu N_2} \doteq \begin{cases} G_2\rho^{-\mu N_2}, & N_1 > N_2 \\ (G_1+G_2)\rho^{-\mu N_1}, & N_1 = N_2 \\ G_1\rho^{-\mu N_1}, & N_1 < N_2 \end{cases} \tag{63}$$

$$ABEP_{\mathrm{1r,FD,PA}} \le (2+F)^{N_{\mathrm{R},r}} \sum_{q_1=0}^{N_{\mathrm{R,r}}} G_1 K_1(q_1)\rho_{\mathrm{All}}^{-N_{\mathrm{R},r}+q_1(1-\mu)} \tag{66}$$

$$ABEP_{\mathrm{r2,FD,PA}} \le \left(\frac{F}{2+F}\right)^{-N_{\mathrm{R,2}}} \sum_{q_2=0}^{N_{\mathrm{R,2}}} G_2 K_2(q_2) 2^{-q_2(1-\mu)} \rho_{\mathrm{All}}^{-N_{\mathrm{R,2}}+q_2(1-\mu)} \tag{67}$$

$$\frac{\partial ABEP_{\mathrm{FD,PA}}}{\partial F} = A_{\mathrm{1r}}(2+F)^{N_{\mathrm{R},r}-1} - A_{\mathrm{r2}}(2+F)^{N_{\mathrm{R,2}}-1}F^{-N_{\mathrm{R,2}}-1} = 0 \tag{68}$$

[11] M. Di Renzo and H. Haas, "Bit error probability of space modulation over Nakagami-m fading: Asymptotic analysis," *IEEE Commun. Lett.*, vol. 15, no. 10, pp. 1026-1028, 2011.

[12] M. Di Renzo and H. Haas, "Improving the performance of space shift keying (SSK) modulation via opportunistic power allocation" *IEEE Commun. Lett.*, vol. 14, no. 6, pp. 500-502, 2010.

[13] A. Younis et al., "Performance of spatial modulation using measured real-world channels," in Proc. *IEEE VTC-Fall*, 2013.

[14] N. Serafimovski, et al., "Practical implementation of spatial modulation," *IEEE Trans. Veh. Technol.*, vol. 62, no.9, pp. 4511-4523, 2013.

[15] J. Zhang, et al., "Bit error probability of spatial modulation over measured indoor channels," *IEEE Trans. Wirel. Commun.*, vol. 13, no. 3, pp. 1380-1387, 2014.

[16] J. Zhang, et al., "Performance of spatial modulation with constant transmitted power under LOS and NLOS scenarios," in Proc. *IEEE ICC*, 2015.

[17] Y. Yang and S. Aissa, "Information-guided transmission in decode-and-forward relaying systems: Spatial exploitation and throughput enhancement," *IEEE Trans. Wireless Commun.*, vol. 10, no. 7, pp. 2341-2351, 2011.

[18] R. Mesleh,et al. "Performance analysis of space shift keying with amplify and forward relaying," *IEEE Commun. Lett.*, vol. 15, no. 12, pp. 1350-1352, 2011.

[19] N. Serafimovski, et al. "Dual-hop spatial modulation (Dh-SM)," in Proc. *IEEE VTC-Spring*, 2011.

[20] S. Sugiura, et al., "Coherent versus non-coherent decode-and-forward relaying aided cooperative space-time shift keying," *IEEE Trans. Commun.*, vol. 59, no. 6, pp. 1707-1719, 2011.

[21] S. Narayanan, et al. "Distributed space shift keying for the uplink of relay-aided cellular networks," in Proc. *IEEE CAMAD*, 2012.

[22] R. Y. Mesleh, et al. "Performance analysis of space shift keying (SSK) modulation with multiple cooperative relays," *EURASIP J. Advances Signal Processing*, 2012.

[23] P. Som and A. Chockalingam, "Bit error probability analysis of SSK in DF relaying with threshold-based best relay selection and selection combining," *IEEE Commun. Lett.*, vol. 18, no. 1, pp. 18-21, 2014.

[24] S. Narayanan, et al. "Distributed spatial modulation for relay networks," in Proc. *IEEE VTC-Fall*, 2013.

[25] M. Zhang, et al. "Differential spatial modulation for dual-hop amplify-and-forward relaying," in Proc. *IEEE ICC*, 2015.

[26] J. Zhang, et al., "On the error probability of spatial modulation over keyhole MIMO channels," *IEEE Comm. Letters*, vol. 17, no. 12, pp. 2221-2224, 2013.

[27] S. Narayanan, et al., "Distributed spatial modulation: a cooperative diversity protocol for half-duplex relay-aided wireless networks," *IEEE Trans. Veh. Technol.*, vol. 65, no. 5, pp. 2947-2964, 2016.

[28] A. Sabharwal, et al., "In-band full-duplex wireless: challenges and opportunities," *IEEE J. Sel. Area. Commun.,* vol. 32, no. 9, pp. 1637-1652, 2014.

[29] Z. Zhang, et al., "Full-duplex wireless communications: challenges, solutions, and future research directions," *IEEE Proc.*, vol. 104, no. 7, pp. 1369-1409, 2016.

[30] P Ju, et al., "An effective self-interference cancellation scheme for spatial modulated full duplex systems," in Proc. *IEEE ICC*, pp. 2123-2128, 2015.

[31] B. Jiao, et al., "Spatial modulated full duplex," *IEEE Wireless Commun. Lett.*, , vol. 3, no. 6, pp. 641-645, 2014.

[32] S. Narayanan, et al.,"Simultaneous uplink/downlink transmission using full-duplex single-RF MIMO," *IEEE Wireless Commun. Lett.*, vol. 5, no. 1, pp. 88-91, 2016.

[33] P. Popovski and H. Yomo, "Wireless network coding by amplify-andforward for bi-directional traffic flows," *IEEE Commun. Lett.*, vol. 11, no. 1, pp. 16-18, 2007.

[34] Q. Li, et al., "Adaptive two-way relaying and outage analysis," *IEEE Trans. Wireless Commun.*, vol. 8, no. 6, pp. 3288-3299, 2009.

[35] R. H. Y. Louie, et al., "Practical physical layer network coding for two-way relay channels: Performance analysis and comparison," *IEEE Trans. Wireless Commun.*, vol. 9, no. 2, pp. 764-777, 2010.

[36] L. Song, "Relay selection for two-way relaying with amplify-and-forward protocols," *IEEE Trans. Veh. Technol.*, vol. 60, no. 4, pp. 1954-1959, 2011.

[37] P. K. Upadhyay and S. Prakriya, "Performance of two-way opportunistic relaying with analog network coding over Nakagami-m fading," *IEEE Trans. Veh. Technol.*, vol. 60, no. 4, pp. 1965-1971, 2011.

[38] H. Cui, et al. "Relay selection for two-way full duplex relay networks with amplify-and-forward protocol," *IEEE Trans. Commun.* vol. 13, no. 7, pp. 3768-3777, 2014.

[39] M. Wen, et al. "Use of SSK modulation in two-way amplify-and-forward relaying," *IEEE Trans. Veh. Technol.*, vol. 63, no. 3, pp. 1498-1504, 2014.

[40] X. Xie, et al. "Spatial modulation in two-way network coded channels: Performance and mapping optimization," in Proc. *IEEE PIMRC*, 2012.

[41] K. Unnikrishnan and B. Rajan, "Space-time coded spatial modulated physical layer network coding for two-way relaying," *IEEE Trans. Wireless Commun.*, vol. 14, no. 1, pp. 331-342, 2015.

[42] I. Krikidis, et al., "Full-duplex relaying over block fading channel: A diversity perspective," *IEEE Trans. Wireless Commun.,* vol. 11, no. 12, pp. 4524-4535, 2012.

[43] M. K. Byun, et al., "Performance and distance spectrum of space-time codes in fast rayleigh fading channels," *IEEE Trans. Commun.* vol. 56, no. 12, pp. 2105-2115, 2008.

[44] Q. Li, et al., "Cooperative two-path relay channels: performance analysis using a markov framework," in Proc. *IEEE ICC*, pp. 3573-3578, 2015.

[45] Q. Li, et al., "Outage analysis of co-operative two-path relay channels," *IEEE Trans. Wireless Commun.*, vol. 15, no. 5, pp. 3157-3169, 2016.

[46] J. N. Laneman, et al., "Cooperative diversity in wireless networks: efficient protocols and outage behavior," *IEEE Trans. Inf. Theory*, vol. 50, no. 12, pp. 3062-3080, 2004.

[47] G. Kramer, et al., "Cooperative strategies and capacity theorems for relay networks," *IEEE Trans. Inf. Theory*, vol. 51, no. 9, pp. 3037-3063, 2005.

[48] M. Duarte, et al., "Experiment-driven characterization of full-duplex wireless systems," *IEEE Trans. Wireless Commun.,* vol. 11, no. 12, pp. 4296-4307, 2012.

[49] T. Riihonen, et al., "Mitigation of loopback selfinterference in full-duplex MIMO relays," *IEEE Trans. Signal Process.,* vol. 59, no. 12, pp. 5983-5993, 2011.

[50] M. Duarte and A. Sabharwal, "Full-duplex wireless communications using off-the-shelf radios: feasibility and first results," in Proc. *IEEE Asilomar*, pp. 1558-1562 2010.

[51] T. Kwon, et al., "Optimal duplex mode for DF relay in terms of the outage probability," *IEEE Trans. Veh. Technol.*, vol. 59, no. 7, pp. 3628-3634, 2010.

[52] Q. Li, et al. "Performance analysis of multi-path relay channels with source power adaptation," in Proc. *IEEE PIMRC*, pp. 23-28, 2015.

[53] Q. Li, et al."Outage analysis of cooperative multi-path relay channels with virtual full-duplex relaying," in Proc. *IEEE ICCW*, pp. 925-930, 2015.

[54] J. Rodriguez, et al. "Performance of full-duplex AF relaying in the presence of residual self-interference,"*IEEE J. Sel. Areas Commun.*, vol. 32, no. 9, pp. 1752-1764, 2014.

[55] Q. Li, et al., "Performance of virtual full-duplex relaying on cooperative multi-path relay channels," *IEEE Trans. Wireless Commun.*,, vol. 15, no. 5, pp. 3628-3642, 2016.

[56] K. Song, et al., "Performance analysis of antenna selection in two-way relay networks," *IEEE Trans. Signal Process.*, vol. 63, no. 10, pp. 2520-2532, 2015.

[57] X. Ge, et al., "5G Ultra-Dense Cellular Networks," *IEEE Wirel. Commun.*, vol. 23, No. 1, pp.72-79, 2016.

[58] D. A. Basnayaka, et al., "Massive but few active MIMO," *IEEE Trans. Vehicular Tech.*, to appear.

[59] G. Amarasuriya, et al.,"Two-way amplify-and-forward multiple-input multiple-output relay networks with antenna selection," *IEEE J. Sel. Areas Commun.*, vol. 30, no. 8, pp. 1513-1529, 2012.

[60] M. S. Alouini and A. Goldsmith, "A unified approach for calculating error rates of linearly modulated signals over generalized fading channels," *IEEE Trans. Commun.*, vol. 47, no. 9, pp. 1324-1334, 1999.

[61] "Encyclopedia of math," [Online] https://www.encyclopediaofmath.org/index.php/Newton_method.

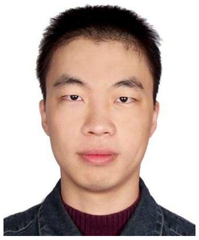

Jiliang Zhang (M'15) received the M.S. and Ph.D. degrees from the Harbin Institute of Technology (HIT) in 2009 and 2014, respectively. He is currently a postdoctoral with the Shenzhen Graduate School, HIT, Shenzhen, China. During this work, he was a visiting scholar with the Communications Group, Department of Electronic and Electrical Engineering, University of Sheffield, U.K., where he was financially supported by the European Commission FP7 project. Since 2014, he has been awarded 3 grants by the NSFC, the Shenzhen government and industry. His research interests cover a wide range of topics in wireless systems, in particular including MIMO channel measurement and modelling, single radio frequency MIMO system, lattice coding, full-duplex relay system, and wireless ranging system.

Qiang Li (M'16) received the B.Eng. degree in communication engineering from the University of Electronic Science and Technology of China (UESTC), Chengdu, China, in 2007 and the Ph.D. degree in electrical and electronic engineering from Nanyang Technological University (NTU), Singapore, in 2011. From 2011 to 2013, he was a Research Fellow with Nanyang Technological University. Since 2013, he has been an Associate Professor with Huazhong University of Science and Technology, Wuhan, China. He was a visiting scholar at the University of Sheffield, Sheffield, UK from March to June 2015. His current research interests include future broadband wireless networks, software-defined networking, content caching, cooperative communications, and cognitive spectrum sharing.

Kyeong Jin Kim (SM'11) received the M.S. degree from Korea Advanced Institute of Science and Technology Technology (KAIST), Daejeon, South Korea, in 1991, and the M.S. and Ph.D. degrees in electrical and computer engineering from the University of California, Santa Barbara, Santa Barbara, CA, USA in 2000. From 1991 to 1995, he was a Research Engineer with the Video Research Center of Daewoo Electronics, Ltd., South Korea. In 1997, he joined the Data Transmission and Networking Laboratory, University of California, Santa Barbara. After receiving his degrees, he joined the Nokia research center (NRC) and Nokia Inc., Dallas, TX, USA, as a Senior Research Engineer, where he was, from 2005 to 2009, an L1 specialist. During 2010-2011, he was an Invited Professor with Inha University, Incheon, South Korea. Since 2012, he has been working as a Senior Principal Research Staff in the Mitsubishi Electric Research Laboratories (MERL), Cambridge, MA. His research interests include transceiver design, resource management, scheduling in the cooperative wireless communications systems, cooperative spectrum sharing system, physical layer secrecy system, and device-to-device communications.

Dr. Kim currently serves as an Editor for the IEEE COMMUNICATIONS LETTERS and *International Journal of Antennas and Propagation*. He also served as a Guest Editor for the *EURASIP Journal on Wireless Communications and Networking*: Special Issue on "Cooperative Cognitive Networks" and *IET Communications*: Special Issue on "Secure Physical Layer Communications". Since 2013, he has served as the TPC Chair for the IEEE GLOBECOM Workshop on Trusted Communications with Physical Layer Security.

Yang Wang received his Ph.D. degree from Harbin Institute of Technology in 2005. From 2005 to 2007, he was a postdoctoral at Harbin Institute of Technology Shenzhen Graduate School, Shenzhen, China. He is currently an associate professor and doctoral supervisor of Harbin Institute of Technology Shenzhen Graduate School. He is a senior member of Chinese Institute of Electronics. Since 2009, he has been awarded 7 grants. He served as the general chair for the 2012 IEEE International Conference on Microwave and Millimeter Wave Technology (IEEE ICMMT 2012). His research interests include wireless communications, UWB system, MIMO system, signal processing and cooperative communications. He has published more than 30 papers in refereed journals and conference proceedings and has been granted about 15 patents in China.

Xiaohu Ge (M'09-SM'11) is currently a full Professor with the School of Electronic Information and Communications at Huazhong University of Science and Technology (HUST), China. He is an adjunct professor with with the Faculty of Engineering and Information Technology at University of Technology Sydney (UTS), Australia. He is the director of China international joint research center of green communications and networking. He received his PhD degree in Communication and Information Engineering from HUST in 2003. He has worked at HUST since Nov. 2005. Prior to that, he worked as a researcher at Ajou University (Korea) and Politecnico Di Torino (Italy) from Jan. 2004 to Oct. 2005. His research interests are in the area of mobile communications, traffic modeling in wireless networks, green communications, and interference modeling in wireless communications. He has published more than 110 papers in refereed journals and conference proceedings and has been granted about 15 patents in China. He received the Best Paper Awards from IEEE Globecom 2010.

Dr. Ge is the vice chair of IEEE Communications Society 5G mobile wireless internet emerging technologies subcommittee. He has been actively involved in organizing more the ten international conferences since 2005. He served as the general chair for the 2015 IEEE International Conference on Green Computing and Communications (IEEE GreenCom 2015). He serves as an Associate Editor for the *IEEE ACCESS*, *Wireless Communications and Mobile Computing Journal (Wiley)* and *the International Journal of Communication Systems (Wiley)*, etc. Moreover, he served as the guest editor for *IEEE Communications Magazine* Special Issue on 5G Wireless Communication Systems.

Jie Zhang is full professor and has held the Chair in Wireless Systems at the Department of Electronic and Electrical Engineering, University of Sheffield (www.sheffield.ac.uk) since 2011. He is a visiting professor at Chongqing University of Posts and Telecommunications and East China University of Science and Technology. He received Ph.D in 1995 and became a Lecturer, Reader and Professor in 2002, 2005 and 2006 respectively. He and his students/colleagues have pioneered research in femto/small cell and HetNets and published some of the earliest and/or most cited publications in these topics. Since 2005, he has been awarded over 20 grants by the EPSRC, the EC FP6/FP7/H2020 and industry, including some of worlds earliest research projects on femtocell/HetNets. He co-founded RANPLAN Wireless Network Design Ltd. (www.ranplan.co.uk) that produces a suite of world leading in-building DAS, indoor-outdoor small cell/HetNet network design and optimisation tools iBuildNetr that have been used by Ericsson, Huawei and Cisco, etc.